High throughput screening and identification of coagulopathic snake venom proteins and peptides using nanofractionation and proteomics approaches

Julien Slagboom[a,b], Marija Mladić[c], Chunfang Xie [b], Freek Vonk[d], Govert W. Somsen[b], Nicholas R. Casewell[a], Jeroen Kool[b]

[a]Centre for Snakebite Research & Interventions, Liverpool School of Tropical Medicine, Liverpool, UK

[b]Division of BioAnalytical Chemistry, Amsterdam Institute for Molecules Medicines and Systems, VU University Amsterdam, Amsterdam, The Netherlands

[c]Animal Sciences and Health, Institute of Biology Leiden, Leiden University, Leiden, The Netherlands

[d]Naturalis Biodiversity Center, Leiden, The Netherlands

[*]Corresponding author j.kool@vu.nl

Abstract

Snakebite is a neglected tropical disease that results in a variety of systemic and local pathologies in envenomed victims and is responsible for around 138,000 deaths every year. Many snake venoms cause severe coagulopathy that makes victims vulnerable to suffering life-threating haemorrhage. The mechanisms of action of coagulopathic snake venom toxins are diverse and can result in both anticoagulant and procoagulant effects. However, because snake venoms consist of a mixture of numerous protein and peptide components, high throughput characterizations of specific target bioactives is challenging. In this study, we applied a combination of analytical and pharmacological methods to identify snake venom toxins from a wide diversity of snake species that perturb coagulation. To do so, we used a high-throughput screening approach consisting of a miniaturised plasma coagulation assay in combination with a venom nanofractionation approach. Twenty snake venoms were first separated using reversed-phase liquid chromatography, and a post-column split allowed a small fraction to be analyzed with mass spectrometry, while the larger fraction was collected and dispensed onto 384-well plates before direct analysis using a plasma coagulation assay. Our results demonstrate that many snake venoms simultaneously contain both procoagulant and anticoagulant bioactives that contribute to coagulopathy. In-depth identification analysis from seven medically-important venoms, via mass spectrometry and nanoLC-MS/MS, revealed that phospholipase A_2 toxins are frequently identified in anticoagulant venom fractions, while serine protease and metalloproteinase toxins are often associated with procoagulant bioactivities. The nanofractionation and proteomics approach applied herein seems likely to be a valuable tool for the rational development of next-generation snakebite treatments by facilitating the rapid identification and fractionation of coagulopathic toxins, thereby enabling specific targeting of these toxins by new therapeutics such as monoclonal antibodies and small molecule inhibitors.

Author summary

Snakebite is a neglected tropical disease that results in more than 100,000 deaths every year. Haemotoxicity is one of the most common signs of systemic envenoming observed after snakebite, and many snake venoms cause severe impairment of the blood coagulation that makes victims vulnerable to suffering life-threating hemorrhage. In this study, we applied a combination of analytical and pharmacological methods to identify snake venom toxins from a wide diversity of snake species that interfere with blood coagulation. Twenty snake venoms were screened for their effects on the blood coagulation cascade and based on the initial results and the medical relevance of the species, seven venoms were selected for in-depth analysis of the responsible toxins using advanced identification techniques. Our findings reveal a number of anticoagulant toxins that have not yet been reported before as such. The methodology described herein not only enables the identification of both known and unknown toxins that cause impairment of the blood coagulation, but offers a throughput platform to effectively screen for inhibitory molecules relevant for the development of next generation snakebite treatments.

1. Introduction

Snakebite is a medically important neglected tropical disease, with up to 5.5 million people bitten annually (1). These bites result in as many as 1.8 million envenomings and 138,000 deaths each year, with three to five times that number of people said to suffer from long term morbidity (1-4). It is the rural poor agricultural workers (e.g. farmers, herdsmen, etc) of the tropics and sub-tropics who suffer the greatest burden of snakebite, with incidences and case fatality rates highest in south and south-east Asia and sub-Saharan Africa (1). In part this is due to socioeconomic reasons, as victims in these parts of the world often do not have rapid access to specialized medical care due to limited health and logistical infrastructure (5), which severely restricts access to snakebite therapy. The only specific therapy available for treating snake envenoming is antivenom. Antivenom comprises polyclonal antibodies, which are purified from the blood of horses or sheep immunised with small, sub-toxic, amounts of snake venom. A proportion of the resulting IgG antibodies are specific to the venom toxins used for immunisation, and thus rapidly neutralize their activity when these therapies are delivered intravenously to patients, particularly if treatment occurs soon after a bite. However, despite these products saving thousands of lives every year, they possess a number of technical limitations that ultimately restrict their clinical utility. Antivenoms exhibit limited paraspecific efficacy (with efficacy restricted mostly to the species used for immunisation), have poor dose efficacy (only 10-20% of antivenom antibodies are typically specific to the toxin immunogens) and exhibit high incidences of adverse effects (which can be as high as in 75% of cases) (6-8). Critically, these therapies are expensive, ranging from $50-350 per vial in Africa, for example (6). Often, treating a snakebite can require multiple vial (e.g. up to 10-20), which makes these therapies unaffordable to the majority of snakebite victims, and pushes those individuals further into poverty. The consequences are poor uptake of this product, weak demand, a lack of manufacturing incentive, and a cycle of undersupply of affordable efficacious antivenom to the regions where it is needed most (9). Consequently, the development of alternative low-cost, low dose, safe and paraspecifically efficacious antivenoms would be of great benefit to snakebite victims inhabiting impoverished regions of the world (10).

Snake venoms consist of a mixture of different protein and peptides that are used to kill, immobilise or incapacitate their prey (11). These ‘toxins’ vary at every taxonomic level and cause a range of different

toxicities, including haemotoxic, neurotoxic and/or cytotoxic pathologies (12-14). The majority of snakebite deaths are thought to be caused by snakes whose venoms are predominately haemotoxic, usually resulting in haemorrhage and perturbations of the clotting cascade. Indeed, venom induced consumption coagulopathy (VICC) is said to be one of the most medically important pathologies caused by snakebite, as it leaves patients highly vulnerable to life-threatening haemorrhage (15). VICC is caused by the continual activation of the clotting pathway via procoagulant toxins present in snake venom, ultimately leading to a depletion of clotting factors (particularly fibrinogen) via their consumption, and incoagulable blood [4]. The majority of snake species that are known to cause VICC are vipers, however, certain Australian elapid snakes, and a small number of colubrid and natricine snakes from Africa and Asia have also been reported to possess procoagulant toxins capable of causing VICC in snakebite victims (7, 15).

Although there are a number of different toxins responsible for causing VICC, many are thought to be members of the snake venom serine protease (SVSPs) and snake venom metalloproteinase (SVMPs) toxin families (5). These toxins activate the blood clotting cascade via their activity on a variety of different clotting factors, of which several are found towards the end of the clotting cascade, including factor V, factor X and prothrombin (factor II). In the same venom, it is not uncommon for other toxins to directly target fibrinogen, resulting in either its degradation or the promotion of weak fibrin clots (7, 11, 15). In addition to procoagulant toxins, snake venoms have also been reported to contain proteins with anticoagulant properties, such as phospholipases A_2s (PLA_2s) and C-type lectin-like proteins (16-18). As mentioned earlier, venom variation is ubiquitous among snake species, and thus the different snake species that cause VICC are thought to have differing numbers of pro- and anti-coagulant toxins in their venom, which may target different components of the blood clotting cascade, even if the pathological outcome in a victim (e.g. VICC) is the same. This variation of venom constituents makes it particularly challenging to develop generic antivenom that could be used to treat snakebite across the world. Thus, identifying the key toxins from different medically-important snake species that are responsible for causing life-threatening coagulopathies would enable us to take an informed approach to generating new, targeted, therapies for snakebite.

Recently we developed a 384 well plate-reader based plasma coagulation assay (19), which gave us the opportunity to perform high-throughput profiling of haemotoxic snake venoms. In addition, we developed an

106 'at-line' nanofractionation setup for high-throughput venom screening of individual components in crude
107 venoms towards selected bioactivities (20, 21). Briefly, crude snake venoms are first separated with liquid
108 chromatography, followed by a post-column split, which gives the opportunity of mass spectrometry (MS)
109 detection in parallel to high-resolution nanofractionation (i.e. 6s per well) onto 384-well plates for
110 bioassaying. Subsequently, bioactivity chromatograms can be constructed by plotting the readout of each
111 well against the time of the corresponding fraction, and when coupled to our coagulation assay, these
112 chromatograms show peaks with positive (i.e. pro-coagulation) or negative (i.e. anti-coagulation) maxima
113 for each bioactive compound (19). Because each bioactivity chromatogram has a corresponding MS
114 chromatogram obtained in the parallel measurement, the accurate masses of the bioactive peaks can be
115 determined when correlating the peaks from the bioassay chromatograms with the data obtained from MS.
116 Thus, this approach enables us to separate snake venom into fractions, and identify the proteins present in
117 those fractions that cause coagulopathic effects in the bioassay.

118 In this study, we selected venoms from 20 different snake species, covering a broad geographical
119 distribution and different taxonomic families, known to interfere with the blood clotting cascade, and we
120 screened them using the described nanofractionation approach to detect their pro- and anti-coagulant
121 activities. Subsequently, we selected seven of these venoms for detailed characterization analysis whereby
122 wells containing bioactive compounds were subjected to tryptic digestion for full protein identification via
123 proteomics. Our methodological approach represents a rapid and straightforward method for identifying pro-
124 and anti-coagulant toxins in snake venoms in a throughput manner. In line with the cumulative literature,
125 our findings show that PLA_2 toxins are frequently detected as anticoagulant bioactive toxins across the
126 species tested, while serine proteases and metalloproteinases are common constituents of procoagulant
127 venom fractions. Thus, this methodology facilitates the identification of both known and unknown
128 coagulopathic toxins, and provides an amenable and targeted approach for testing the neutralisation of
129 pathogenic snake venom toxins by next generation antivenoms.

130

2. Materials and Methods

2.1. Chemicals and stock solutions

The solvents and chemicals used in this research were of analytical grade. Acetonitrile (ACN) and formic acid (FA) were purchased from Biosolve (Valkenswaard, The Netherlands) and water was purified using a Milli-Q plus system (Millipore, Amsterdam, The Netherlands). Bovine plasma was obtained from Biowest (Amsterdam, The Netherlands). Iodoacetamide, β-mercaptoethanol, Argatroban, Ammonium bicarbonate and calcium chloride, were obtained from Sigma-Aldrich (Zwijndrecht, The Netherlands). Sequencing grade modified trypsin was purchased from Promega Benelux B.V. (Leiden, The Netherlands), and stored and handled according to the manufacturer's instructions. The snake venom pools used in this study *Echis ocellatus* (Nigeria), *Echis carinatus* (India), *Echis carinatus* (UAE), *Echis pyramidum leakeyi* (Kenya), *Echis coloratus* (Egypt), *Crotalus horridus* (USA), *Macrovipera lebetina* (Uzbekistan), *Daboia russelli* (Sri Lanka), *Bothrops asper* (Costa Rica), *Bothrops jararaca* (Brazil), *Lachesis muta* (Brazil), *Bothriechis schlegelii* (Costa Rica), *Calloselasma rhodostoma* (captive bred, Thailand ancestry), *Hypnale hypnale* (Sri Lanka), *Trimeresurus albolabris* (Thailand), *Trimeresurus stejnegeri* (Malaysia), *Deinagkistrodon acutus* (China), *Dispholidus typus* (South Africa), *Rhabdophis subminiatus* (Hong Kong) and *Oxyuranus scutellatus* (Papua New Guinea). They were sourced in house from animals held in, or historical venoms stored in, the herpetarium at the Liverpool School of Tropical Medicine, UK. These species were selected based on previous reports of coagulopathic venom activity (7, 19, 22, 23). Venoms were in lyophilized form at 4°C, until reconstitution in water to make 5 mg/mL stock solutions, which were then aliquoted and stored at –80°C until use.

2.2. Ethics statement

The maintenance and handling of venomous snakes was undertaken following approvals granted by the Animal Welfare and Ethical Review Board of the Liverpool School of Tropical Medicine and the UK Home Office (licence #X2OA6D134), and thus meet the national and legal ethical requirements set by the Government of the United Kingdom (under the Animal and scientific procedures act 1986) and EU directive 2010/63/EU.

2.3. Liquid chromatography, at-line nanofractionation and mass spectrometry

Liquid chromatography separation, parallel at-line nanofractionation and subsequent mass spectrometry analyses were performed in an automated fashion. A Shimadzu UPLC system ('s Hertogenbosch, The Netherlands) was used for the LC separation. All the settings of the system were controlled with Shimadzu Lab Solutions software. Fifty microlitres of each sample was injected by a Shimadzu SIL-30AC autosampler, and the two Shimadzu LC-30AD pumps were set to a total flow rate of 500 µl/min. A 250×4.6 mm Waters Xbridge Peptide BEH300 C_{18} analytical column with a 3,5-µm particle size and a 300-Å pore size was used for separation of the venoms. The separations were performed at 30 °C in a Shimadzu CTD-30A column oven. Mobile phase A comprised of 98% H_2O, 2% ACN and 0.1% FA, and mobile phase B comprised of 98% ACN, 2% H_2O and 0.1% FA. A linear increase of mobile phase B from 0% to 50% in 20 min was followed by a linear increase from 50% to 90% B in 4 min and a 5 min isocratic separation at 90% B. The starting conditions (0% B) were reached linearly in 1 min and the column was then equilibrated for 10 min at 0% B. The column effluent was split post-column in a 1:9 volume ratio. The larger fraction was sent to a FractioMate™ FRM100 nanofraction collector (SPARK-Holland & VU, Netherlands, Emmen & Amsterdam) or a modified Gilson 235P autosampler. The smaller fraction was sent to the Shimadzu SPD-M30A photodiode array detector followed by an Impact II QTOF mass spectrometer (Bruker Daltonics, Billerica, MA, USA). An electrospray ionization source (ESI) was equipped onto the mass spectrometer and operated in positive-ion mode. The ESI source parameters were: capillary voltage 4.5 kV, source temperature 180°C, nebulizer at 0.4 Bar and dry gas flow 4 L/min. MS spectra were recorded in the *m/z* 50–3000 range and 1 average spectrum was stored per s. Bruker Compass software was used for the instrument control and data analysis. LC fractions (1 per 6 s) were collected row by row in serpentine-like fashion on clear 384-well plates (Greiner Bio One, Alphen aan den Rijn, The Netherlands) using the in-house written software Ariadne or FractioMator when the Fractionmate was used, with a maximum of four plates in one sequence. Each chromatographic run was collected into 350 wells of one 384-well plate. After fractionation, the plates were evaporated overnight for approximately 16 h using a Christ Rotational Vacuum Concentrator RVC 2-33 CD plus (Salm en Kipp, Breukelen, The Netherlands). The plates were then stored at –20°C until further use, i.e., either bioassaying or tryptic digestion.

2.4. Plasma coagulation assay

The coagulation cascade interfering properties of snake venoms were analysed using a previously described plasma coagulation assay (19). Briefly, 20 µL of 20 mM calcium chloride solution (room temperature) was dispensed onto a 384-well plate containing LC fractionated snake venom using a Thermo Scientific multidrop 384 reagent dispenser. Next, 20 µL of bovine plasma (room temperature) was dispensed into each well. Finally, the plate was placed into the plate reader and the absorbance was measured kinetically at 595 nM for 80 cycles (± 90 min) at 25°C.

The resulting data was normalized and analysed in three different ways to differentiate between anticoagulant, fast procoagulant and slow procoagulant detected bioactive components First, the last measurement cycle was plotted as a single point measurement to display the anticoagulant compounds. Second, the average slope of cycles 1-5 were plotted to show the fast procoagulant components. Last, the average slope of cycles 1-15 were plotted to show the remainder of the procoagulant components ("slow procoagulants"). The rationale for plotting the procoagulant activity in two different ways is that the fast procoagulant compounds clot the plasma in the wells in a distinct manner, resulting in a rapid rise in absorbance followed by a plateau, and where this plateau typically occurs at a lower overall absorbance than that observed with the "slow procoagulant" components. Thus, wells containing the slower procoagulant components reach an absorbance that surpasses those of the wells containing the fast procoagulants, but over a prolonged period of time.

2.5. Correlating coagulation data with mass spectrometry data

The elution times and peak widths at half maximum of the peaks observed in the bioassay chromatograms were determined. For the corresponding time interval, the average mass spectrum was extracted from the parallel recorded MS chromatogram (total-ion current (TIC)). For all m/z's with a significant signal in this mass spectrum, extracted-ion currents (XICs) were plotted. Based on matching peak shape and retention time, m/z's were assigned to the appropriate bioactive peaks observed in the bioassay chromatogram based. The charge states of the particular one deconvolutes spectra were assigned by the software based on the observed isotope distribution. Finally, deconvolution of the full mass spectra recorded for the assigned peaks provided the accurate monoisotopic masses.

The difference in flow rate of the flow ratio directed to the bioassay and the flow ratio directed to the mass spectrometer after the post-column split caused a constant time delay between the nanofractionated plates and the obtained MS data. To determine the duration of this delay, the thrombin inhibitor argatroban was nanofractionated, resulting in a negative peak in the plasma coagulation assay, which could be correlated to its corresponding known extracted ion current (shown in SI Fig 1). The difference in elution time between the two peaks is the delay between the MS and the nanofractionation collector and was found to be 78 sec. Using the determined delay, the *m/z*-values measured in the MS could be correlated with the bioactive peaks observed in the bioassay chromatograms.

2.6. Identification of coagulopathic toxins via tryptic digestion

After for a specific sample the wells containing bioactive compounds were pinpointed, the same sample was fractionated again, and the content of the active wells was subjected to tryptic digestion in order to identify coagulopathic toxins using a proteomics approach. For that, the plate was first freeze-dried,and then 40 µL of water was added to each selected well, reconstituting the contents for 30 min at room temperature. Next, 10 µL from each rwell was transferred to an Eppendorf tube containing 15 µL of digestion buffer (25 mM ammonium bicarbonate, pH 8.2). Subsequently, 1.5 µl of reducing agent (0.5% β-mercaptoethanol) was added to each tube followed by a 10-min incubation at 95 °C. Then, the samples were cooled to room temperature and centrifuged at 150 RCF for 10 s in a Himac CT 15RE centrifuge. Next, 3 µL of alkylating agent (55 mM iodoacetamide) was added and the mixture was incubated in the dark at room temperature for 30 min. Subsequently, 3 µL of 0.1 µg/µL trypsin was added followed by incubation at 37 °C for 3 h, after which an additional 3 µL of trypsin solution was added to the tube and the samples were incubated overnight. Next, 1 µL of 5% FA was added to quench the digestion, followed by brief centrifugation to remove any particulate matter. Finally, the samples were centrifuged for 10 s at 150 RCF and the supernatants were transferred to autosampler vials with glass inserts and analyzed using nanoLC-MS/MS.

NanoLC separation of the tryptic digests were performed using an UltiMate 3000 RSLCnano system (Thermo Fisher Scientific, Ermelo, The Netherlands). The autosampler was run in full-loop injection mode. The autosampler was set to a 1 µL injection volume and after injection the samples were separated on an analytical capillary column (150 mm x 75 µm) packed in-house with Aqua C_{18} particles (3 µm particle size,

200 Å pores; Phenomenex, Utrecht, The Netherlands). The mobile phase was comprised of eluent A (98% water, 2% ACN, 0.1% FA) and eluent B (98% ACN, 2% water, 0.1% FA). The applied gradient was: 2 min isocratic separation at 5% B, linear increase to 80% B in 15 min, 3 min isocratic separation at 80% B, down to 5% B in 0.5 min and equilibration for 9 min. The column was kept at 30 °C in the column oven. Absorbance detection was performed at 254 nm followed by mass detection using a Bruker MaxisII qTOF mass spectrometer (Bruker, Bremen, Germany) equipped with a nanoESI source operating in positive-ion mode. The ESI source parameters were: source temperature, 200 °C; capillary voltage, 4.5 kV; gas flow, 10 L/min. Spectral data were stored at a rate of 1 average spectrum/s in the range of 50 to 3000 m/z. MS/MS spectra were obtained using collision induced dissociation (CID) in data-dependent mode using 35-eV collision energy. Bruker Compass software was used for instrument control and data analysis.

Using the data obtained for the tryptic digests of the samples, protein identification was carried out using MASCOT (Matrix Science, London, United Kingdom) searches against Swiss-Prot, NCBInr and species-specific databases. The latter were generated from previously published transcriptomic data for those species that were available (24-27) and were used for the identification of venom toxins for which activity was observed. The following search parameters were used: ESI-QUAD-TOF as the instrument type, semiTrypsin as the digestion enzyme allowing for one missed cleavage, carbamidomethyl on cysteine as a fixed modification, amidation (protein C-terminus) and oxidation on methionine as variable modifications, ± 0.05 Da fragment mass tolerance and ± 0.2 Da peptide mass tolerance. To compare the deconvoluted monoisotopic masses with masses found by Mascot we used Uniprot to obtain information about potential PTMs and the presence or absence of pro and signal peptides. Uniprot contains transcriptomic data which usually does not represent the native form of the toxins since it does not take possible PTMs and the absence of pro or signal peptides into account. Therefore toxins were drawn in Chemdraw including the appropriate PTMs and excluding any pro or signal peptides in order to obtain the exact mass to facilitate correlations between XICs and the MS data. The Uniprot database generated a high number of Mascot identities from which a selection was made based on protein score (> 50), sequence coverage (> 20%) and known activity.

2.7. Statistical analysis

Comparisons of the molecular weights of the various procoagulant and anticoagulant venom toxins detected from the seven venoms were performed using the R package Artool (28). The data comprised of the molecular weights of toxin identities found through tryptic digestion and Mascot database searching described above. The full data set of toxin molecular weights can be found in Table 2. As the compiled data was found to be non-Gaussian in distribution, a non-parametric factorial analysis was performed, which was undertaken using the function art() in Artool (28).

3. Results & Discussion

3.1. Coagulopathic activity profiling of snake venoms

The objective of this study was to characterise the coagulopathic activity of various snake venoms and identify their coagulopathic toxins. Our approach consisted of an initial screening strategy, whereby the bioactivity of 20 snake venoms sourced from different taxonomic families and geographic origins were elucidated, followed by in depth proteomic characterization of the active coagulopathic compounds for seven of those venoms. The initial HT screening approach utilized high-resolution LC fractionation of venom (50 µL injections of 5 mg/mL solutions) into a 384-well plate coupled to a plasma coagulation assay. This bioassay measures differences in clotting velocity between control wells which produce a normal clotting profile (e.g. plasma in the presence of calcium chloride), and wells containing bioactive components (i.e. procoagulants or anticoagulants). Plotting the different velocities against the time of the fraction results in positive peaks for procoagulant compounds (where clotting is more rapidly stimulated, resulting in enhanced clotting speed) and negative peaks for anticoagulant compounds (where clotting is reduced or inhibited, resulting in prolonged clotting times or prevention of clotting).

Table 1. Semi-quantitative determination of procoagulant activity of venom of 20 snake species. The extent of pro- and anti-coagulant activity is graded from strong (+++) to weak (+), where 0 represents no activity detected.

Species	Pro	Anti	Species	Pro	Anti
Echis ocellatus	+	0	*Bothriechis schlegelii*	++	++
Echis carinatus	++	++	*Calloselasma rhodostoma*	++	0
Echis carinatus	+	0	*Hypnale hypnale*	++	0
Echis pyramidum leakeyi	+	++	*Trimeresurus albolabris*	+	+
Echis coloratus	+	++	*Trimeresurus stejnegeri*	+	++
Crotalus horridus	+	0	*Deinagkistrodon acutus*	+	0
Macrovipera lebetina	+	++	*Dispholidus typus*	+	0
Daboia russelii	++	+++	*Rhabdophis subminiatus*	0	0
Bothrops asper	+++	+++	*Oxyuranus scutellatus*	0	+++
Bothrops jararaca	++	0	*Lachesis muta*	++	++

Based on the initial screening, the pro- and anti-coagulant activities of the 20 snake venoms were compared semi-quantitatively based on the observed activity (Table 1). For a detailed view of the resulting assay data for each of these venoms we direct the reader to SI Fig 2. Our findings demonstrate a variable pattern of coagulopathic activity among those species at the concentration tested. The majority of the venoms tested demonstrated procoagulant activities, which was anticipated given prior findings (7), although the extent of this activity varied extensively, with *Bothrops asper* providing the most potent effect. Surprisingly, neither *Oxyuranus scutellatus* or *Rhabdophis subminiatus* venoms exhibited evidence of procoagulation under the assay conditions used here, despite prior reports of this venom activity (7, 22). Similarly, we observed extensive variation in anticoagulant venom effects, with three of the 20 species showing maximal effects (Table 1), while we did not detect discernible anticoagulant venom activity for nine of the species. Notably, *B. asper* also exhibited the most potent anticoagulant effects detected (alongside *Daboia russelii* and *Oxyuranus scutellatus*), demonstrating that this venom is highly coagulopathic, and acts via both procoagulant and anticoagulant activities.

Seven venoms (underlined in Table 1) were selected for in depth characterisation. These venoms were selected because they represent snakes of greatest medical importance in their distinct geographic locales (e.g. the viperid species *Echis ocellatus*, *Daboia russelii*, *Bothrops asper*, *B. jararaca*, *Calloselasma rhodostoma*) or because they represent different snake families (e.g. the elapid species *Oxyuranus scutellatus* and the colubrid species *Dispholidus typus*). The results of these optimized experiments demonstrated that all seven of the snake venoms exhibited substantial procoagulant venom activity (Figure 1), broadly consistent with our initial venom screen (Table 1), and recent analyses undertaken using crude venom (7, 22, 29-35). The notable exception to this was that of *O. scutellatus*, which did not exhibit procoagulant activity in our initial screen (Table 1), but did so in these optimized experiments (Figure 1). These latter findings are more consistent with the literature than our earlier experiment (22), and likely reflect the differences in venom concentration (5mg/mL instead of 1mg/mL) and $CaCl_2$ (20 mM instead of 100 mM) used for the subsequent optimized experiments. The decrease of $CaCl_2$ resulted in an assay readout with significantly less baseline noise and therefore increased sensitivity, which combined with increased venom concentration, resulted in the detection of procoagulant venom activity *for O. scutellatus*.

3.2. Proteomic identification of coagulopathic toxins

3.2.1. Correlation of bioactivity peaks with mass spectrometry data

After coagulopathic profiling of the venoms, the first step in identifying the active toxins was to assign accurate masses of individual venom components exhibiting activity in the plasma coagulation assay. This was done by correlating bioactivity chromatograms to the corresponding MS chromatograms. This correlation was based on elution time and peak shape of the bioactive peaks. The data interpretation of the analysis of the seven snake venoms assayed here are shown in figures 1 and 2, and the *m/z*-values and their corresponding masses for all bioactives can be found in table 2. This method proved to be successful for masses up to 15 kDa, however larger toxins showed to be much more difficult to correlate. This was most likely caused by a lack of sensitivity of the LC-MS caused by poor ionization or insufficient amounts of the relevant proteins.

3.2.2. NanoLC-MS/MS analysis of tryptic digests of venom fractions showing bioactivity

In the second step to identify the coagulopathic venom toxins observed in the plasma coagulation assay after fractionation, venoms were re-fractionated and the content of selected wells containing bioactive compounds was subjected to tryptic digestion (see SI Fig 3 for details of well selection for each venom). The digested content of each well was analysed by nanoLC-MS/MS and the data was subjected to a Mascot database search using the Uniprot database and species-specific databases compiled from transcriptomic data. We noted that the search results provided by the Uniprot database provided a large number of Mascot identities at the timeframes of the pro- and anti-coagulant activities. This is likely the result of the bioactive compound not having an exact match in the database due to low toxin representation, but having high sequence similarity to a number of venom toxins found in related snake species. The toxin identities mentioned in the text below were selected based on the sequence coverage, protein score and known functional activity, and the full results are detailed in the SI Uniprot database table in the Supplementary Information. Thereafter, we compared the deconvoluted monoisotopic masses of the XICs correlated with the bioactive peaks (described above) with the masses of the compounds identified via Mascot to assign protein identities found on Uniprot to coagulopathic venom toxins (Table 2). This proved to be again successful for smaller toxin components (<15 kDa), but for larger toxins (e.g. >20kDa) none of the XICs could be correlated to Mascot identities (Table 2).

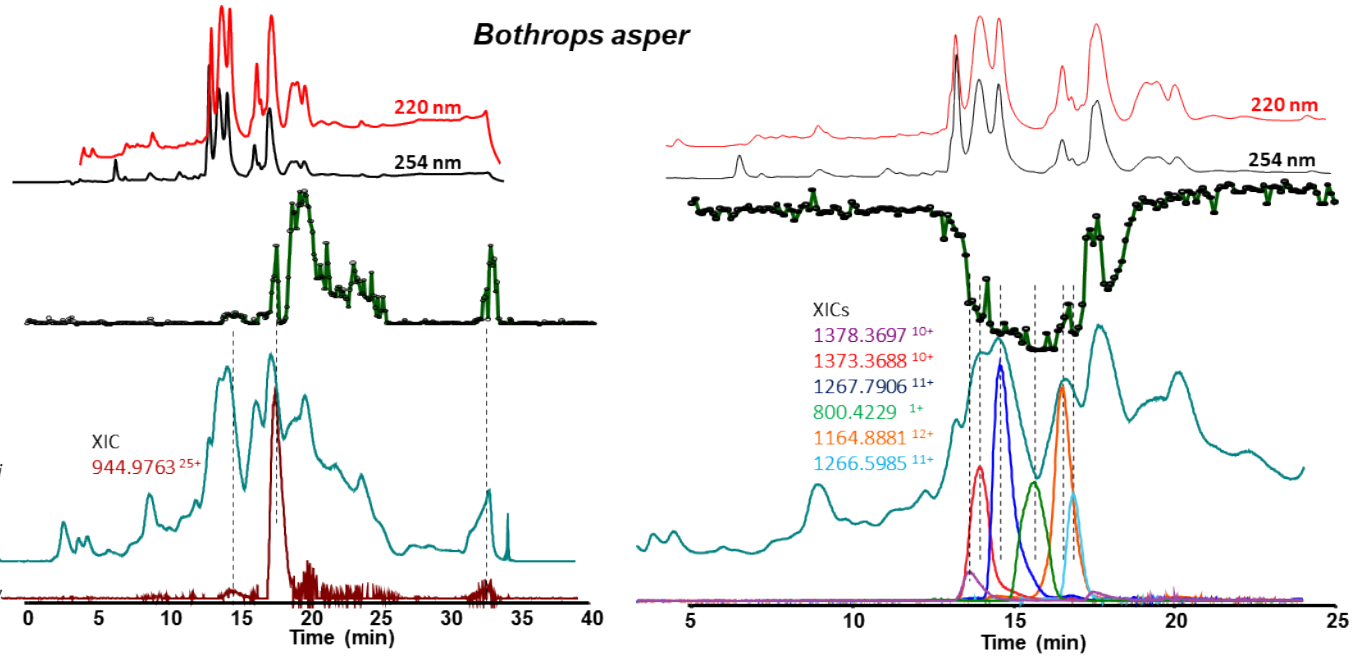

Fig 1. Detection of coagulation interfering compounds of *Bothrops asper* by correlating MS and bioassay data obtained upon LC analysis of crude snake venom (5 mg/mL). *i*: UV chromatograms detected at 220 and 254 nm. *ii*: Bioactivity chromatograms obtained after fractionation by plotting the results of the plasma coagulation assay against time; the positive and negative peaks indicate the presence of procoagulant and anticoagulant bioactive compounds respectively. *iii*: MS chromatograms (TIC), *iv*: Extracted-ion chromatograms (XICs) of *m/z*-values corresponding to bioactive peaks. Further experimental conditions, see Materials and Methods section.

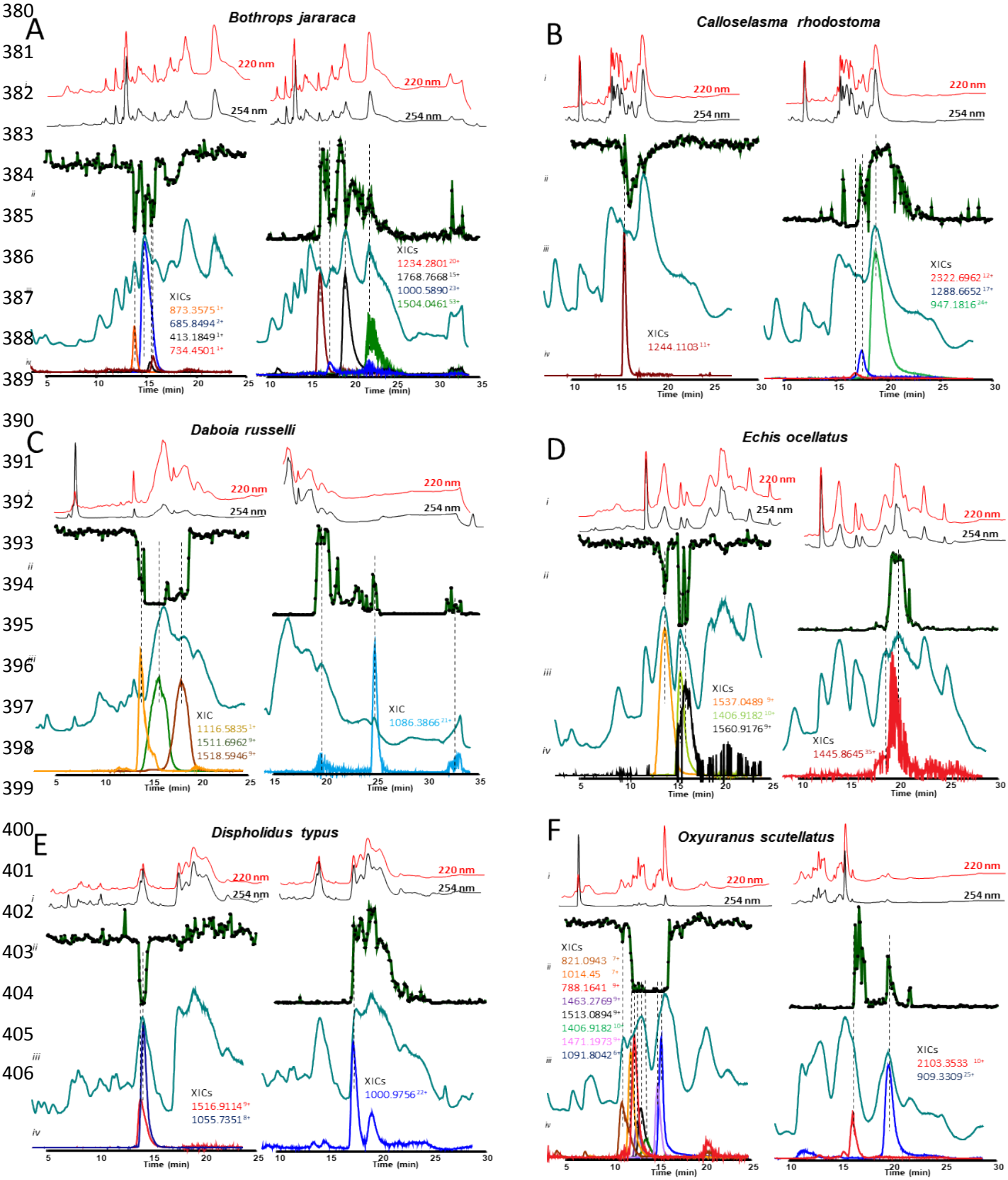

Fig 2. Identification of coagulopathic compounds from the remaining six venoms by correlating MS data with bioassay data. *i*: UV trace of the snake venoms at 220 and 254 nm obtained by LC-MS. *ii*: bioactivity chromatograms obtained by plotting the results of the plasma coagulation assay in Prism software. The peaks with positive (left) and negative (right) maxima indicate the presence of procoagulant and anticoagulant bioactive compounds respectively. 6-s resolution fractions were collected onto 384 well plates by the nanofractionator after 50-µL injection of crude snake venom at a concentration of 5 mg/mL. *iii*: LC-MS chromatograms displaying the total ion current (TIC), *iv*: the extracted ion currents (XICs) of the *m/z*-values corresponding to bioactive peaks found in the MS spectra.

415 **Table 2.** Assignment of coagulopathic venom toxins based on masses detected for intact bioactive
416 components and Mascot hits after tryptic digestion.

417
418

Species	*m/z*-value	MS accurate mass	Mascot protein hits	Mascot exact mass	Toxin class	Activity
Bothrops asper	1378.37 (10+)	13765.58	**PA2H3_BOTAS**	13765.58	PLA_2	Anticoagulant
	1373.37 (10+)	13714.56	**PA2H2_BOTAS**	13714.56	PLA_2	Anticoagulant
	1164.88 (12+)	13957.53	**PA2B3_BOTAS**	13957.49	PLA_2	Anticoagulant
	1267.79 (11+)	13925.58	-	-	-	Anticoagulant
	800.42 (1+)	799.42	-	-	-	Anticoagulant
	1266.60 (11+)	13912.46	**PA2HA_BOTAS***	13896.51	PLA_2	Anticoagulant
	944.98 (25+)	23814.00	-	-	-	Procoagulant
	-	-	**VM1B1_BOTAS**	22735	SVMP	Procoagulant
Bothrops jararaca	873.36 (1+)	872.35	-	-	-	Anticoagulant
	685.85 (2+)	1369.68	-	-	-	Anticoagulant
	413.18 (1+)	412.12	-	-	-	Anticoagulant
	734.45 (1+)	733.44	-	-	-	Anticoagulant
	1234.29 (20+)	24665.60	-	-	-	Procoagulant
	1768.77 (25+)	26531.50	-	-	-	Procoagulant
	1000.59 (23+)	23013.55	-	-	-	Procoagulant
	1504.05 (53+)	79714.44	-	-	-	Procoagulant
	-	-	**VSPA_BOTJA**	25555.45	SVSP	Procoagulant
	-	-	**VSP1_BOTJA**	25087.68	SVSP	Procoagulant
	-	-	**VSP2_BOTJA**	25183.62	SVSP	Procoagulant
	-	-	**SLEA_BOTJA**	15199.29	C-Type lectin	Procoagulant
	-	-	**VM3JA_BOTJA**	46790.97	SVMP	Procoagulant
	-	-	**VM2J2_BOTJA**	30839.23	SVMP	Procoagulant

Calloselasma rhodostoma	1244.11 (11+)	13665.08	**PA2BD_CALRH**	13665.02	PLA_2	Anticoagulant
	2322.70 (12+)	27872.35	-	-	-	Procoagulant
	1288.67 (17+)	21881.17	-	-	-	Procoagulant
	947.18 (24+)	22693.13	-	-	-	Procoagulant
	-	-	**VSPF2_CALRH**	26431.16	SVSP	Procoagulant
	-	-	**VM1K_CALRH**	22966.17	SVMP	Procoagulant
	-	-	**VM2RH_CALRH**	30755.33	SVMP	Procoagulant
Daboia russelli	1511.70 (9+)	13587.22	**PA2B8_DABRR**	13587.20	PLA_2	Anticoagulant
	1116.58 (1+)	1115.58	-	-	-	Anticoagulant
	1518.59 (9+)	13649.25	**PA2B3_DABRR***	13663.18	PLA_2	Anticoagulant
	1086.39 (1+)	22778.91	-	-	-	Procoagulant
Echis ocellatus	1537.05 (9+)	13815.35	**PA2HS_ECHOC**	13815.28	PLA_2	Anticoagulant
	1541.47 (9+)	13856.14	**PA2A5_ECHOC**	13856.07	PLA_2	Anticoagulant
	1560.92 (9+)	14030.16	-	-	-	Anticoagulant
	1445.86 (35+)	52015.87	-	-	-	Procoagulant
	-	-	**VM3E2_ECHOC**	47274.70	SVMP	Procoagulant
	-	-	**VM3E6_ECHOC**	47062.79	SVMP	Procoagulant
	-	-	**SL1_ECHOC**	14080.37	C-Type lectin	Procoagulant
	-	-	**SL124_ECHOC**	14525.60	C-Type lectin	Procoagulant
Dispholidus typus	1516.91 (9+)	13634.10	-	-	-	Anticoagulant
	1055.74 (8+)	8432.80	-	-	-	Anticoagulant
	1000.98 (22+)	22993.99	-	-	-	Procoagulant
Oxyuranus scutellatus	788.16 (9+)	6993.29	**VKT_OXYSC**	6993.29	Kunitz-type serine	Anticoagulant

				protease inhibitor	
1091.80 (6+)	6536.81	**VKT3_OXYSC**	6536.82	Kunitz-type serine protease inhibitor	Anticoagulant
821.09 (7+)	5737.58	-	-	-	Anticoagulant
1014.45 (7+)	7090.32	-	-	-	Anticoagulant
1463.28 (9+)	13151.39	-	-	-	Anticoagulant
1513.09 (9+)	13600.74	-	-	-	Anticoagulant
1406.92 (10+)	14052.06	-	-	-	Anticoagulant
1471.20 (9+)	13222.68	-	-	-	Anticoagulant
2103.35 (10+)	21023.53	-	-	-	Procoagulant
909.33 (25+)	22695.54	-	-	-	Procoagulant
		PA2TA_OXYSC	13805.19	PLA_2	Anticoagulant
		PA2TB_OXYSC	13212.69	PLA_2	Anticoagulant
		PA21_OXYSC	14077.02	PLA_2	Anticoagulant
		PA2TC_OXYSC	13289.79	PLA_2	Anticoagulant

Close match and likely the same toxin due to a post-translational modification

421

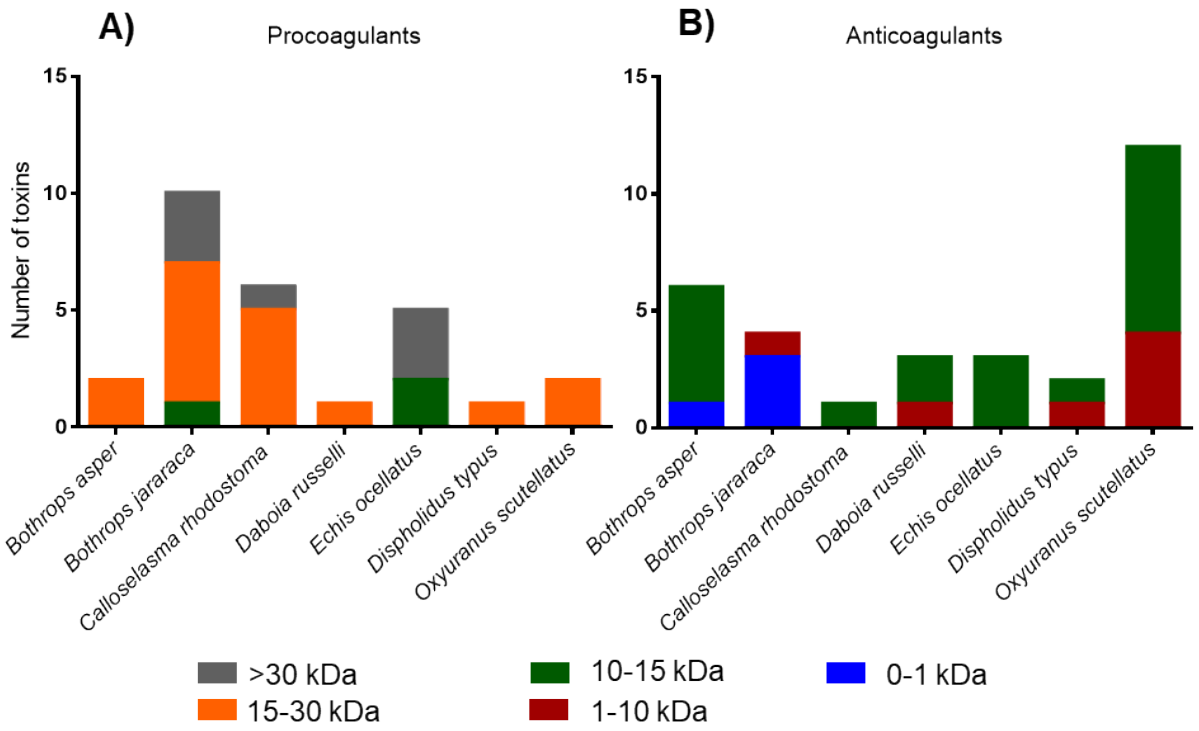

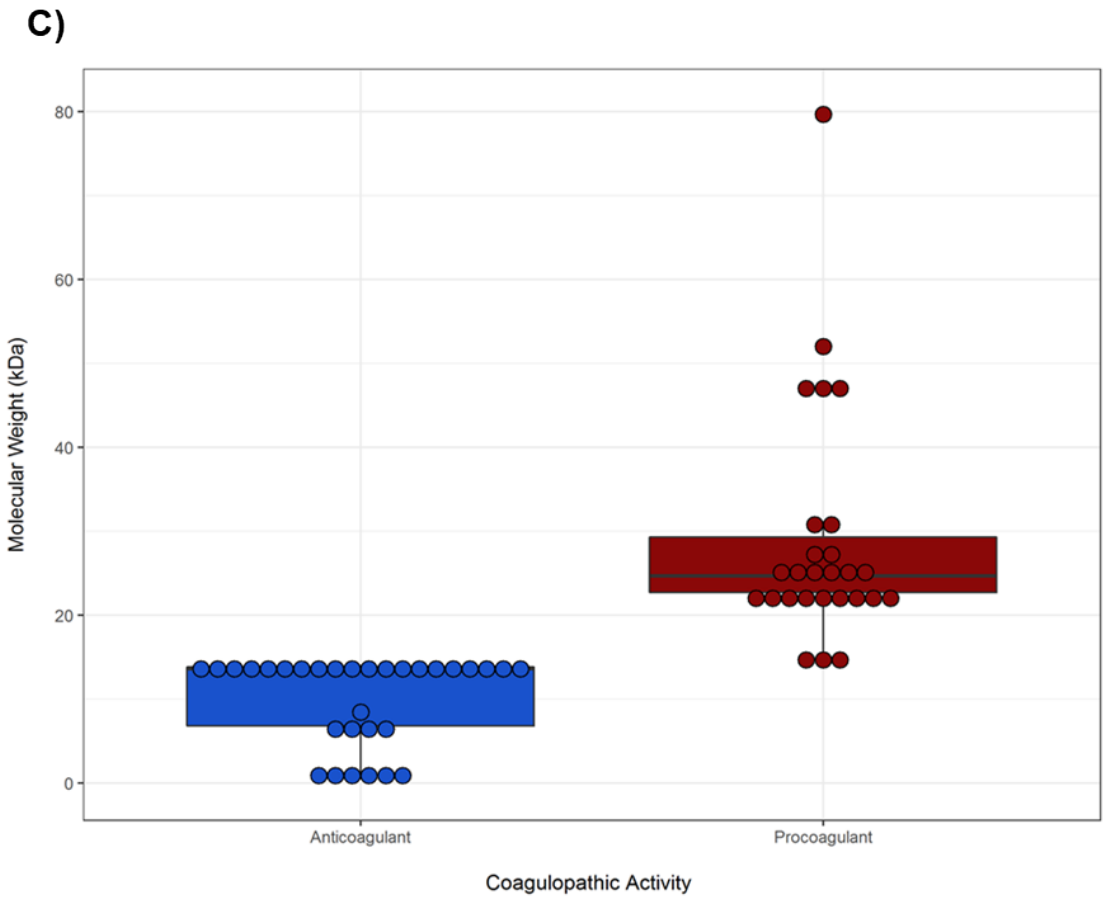

Fig 3. The molecular weight distribution of the various anti- and pro-coagulant toxins identified in the venom of each of the seven snake species. The number and molecular weight range of toxins identified from each snake species are summarized for procoagulant (**A**) and anticoagulant (**B**) bioactives. Toxin identifications are derived from those described in Table 2 and their respective molecular weights were calculated by drawing structures in chemdraw and adding appropriate PTMs. The full data can be found in detail in the SI Uniprot database table. **C**) Molecular weight comparisons of the anticoagulant and procoagulant toxins detected from all seven snake venoms. Boxes show the interquartile range of each dataset, with the boldened horizontal line representing the median value, and each data point is illustrated by a dot. Statistical comparisons, via non-parametric factorial analysis, reveals that procoagulant venom toxins exhibit significantly higher molecular weights than anticoagulants (P = 2.22e-16, F=163.52).

Despite these limitations, summarizing the toxin identities from the Mascot hits and XICs of the various anti- and pro-coagulant venom fractions revealed noticeable differences in the masses of the toxins associated with these two bioactivities (Fig 3. Panel C). In total we detected 59 toxins in the fractions where anticoagulant activities were observed for the seven venoms. The masses ranged from 412 Da to 30 kDa in size, with the majority falling between 1 and 15 kDa. For procoagulant activity we found 38 toxins, which exhibited a much broader mass range, from 11 kDa to 79 kDa. However, the majority of these were larger than 15 kDa in size. Although there are clear inter-specific distributions in the molecular weights of the various coagulopathic toxins identified, statistical analyses reveal that procoagulant venom toxins exhibit significantly higher molecular weights than their anticoagulant counterparts (non-parametric factorial analysis; P = 2.22e-16, F=163.52). In the next sections we detail the toxin identities of the various coagulopathic toxins found in each of the seven venoms.

3.3. Mascot results summary for all seven species

3.3.1 Bothrops asper

On the basis of the *m/z*-values detected for the anticoagulant-active peaks for *Bothrops asper*, six molecular masses were assigned (Figure 1; Table 1). Four of these were found to be proteins of the PLA_2 toxin family. A number of snake venom PLA_2s have previously been described to exert anticoagulant effects via binding to factor Xa and inhibiting prothrombinase activity (36). One of the four PLA_2s detected in our study has previously been described to be anticoagulant, namely "Basic phospholipase A2 homolog 2" (*m/z*-value of 1373.3688^{10+}, which corresponds to an accurate mass of 13714.5639 Da), which has been described to inhibit prothrombinase activity (36). The remaining three PLA_2s have *m/z*-values of 1378.3697^{10+}, 1266.5985^{+11} and 1164.8811^{12+}, which correspond to accurate masses 13765.5821 Da, 13912.4649 Da and 13957.5232 Da, respectively. The first of these identities corresponds to the "PLA_2 Basic phospholipase A2 homolog M1-3-3", which is predicted to exert myotoxic activity based on its similarity to PLA_2s from other snake species (37). The second corresponds to "Basic phospholipase A2 homolog 4a" and exhibits a mass ~16 Da higher than the PLA_2 toxin, and this slight difference may be caused by an oxidation of methionine. This toxin has only previously been described as myotoxic (38). The third PLA_2 corresponds to "Basic phospholipase A2 myotoxin III" which is also only known to exhibit myotoxic activity (38-43). The remaining masses detected to potentially exert anticoagulant activity had an XICs of 800.4229^{1+} and 1267.79^{11+} and accurate masses of 799.4155 and 13925.58 Da, which both remain unidentified. Despite *B. asper* venom exhibiting potent procoagulant activity (e.g. Table 1, Figure 2) only one *m/z*-value could be assigned to components exerting this effect, 944.976325^{+25}, and to which no corresponding match could be found in the Mascot database after proteomics analysis. Nonetheless, given that the mass of this venom toxin was 23.8 kDa, it seem likely that it belongs to the SVMP or SVSP toxin family. Analysis of Mascot identities found at the time frame of the eluted procoagulant activities, detected relatively few toxins, but of those "Snake venom metalloproteinase BaP1" is a known procoagulant SVMP, and thus may be responsible for this observed bioactivity (41).

3.3.2 *Bothrops jararaca*

Despite the association of eight *m/z*-values with coagulopathic venom activity, we were unable to confidently assign any of these venom component masses to Mascot hits. Four of these components corresponded to anticoagulant bioactive peaks in the plasma coagulation assay (Figure 2B), and exhibited masses of 400-1400 Da. These findings contrast starkly with the majority of the anticoagulants identified in the venom of the congeneric species *B. asper* (five anticoagulants 12-14 kDa in size), with two unidentified components from that species (799 and 13925.58 Da) with 799 Da falling within a similar mass range to the anticoagulants identified in *B. jararaca* venom. While some of these low molecular weight components may simply be co-eluting with anticoagulant toxins, it is also possible that the active toxins are indeed co-eluting but are not detected by either MS or Mascot. However, further elucidation of these compounds could be of particular value if they do exhibit anticoagulant activity since the small size of these molecules makes them amenable from a drug discovery perspective. Bradykinin-potentiating peptides match the detected molecular masses and, have previously been characterized for this venom (44, 45). As for *B. asper*, none of the m/z-values associated with procoagulant activity could be matched to Mascot hits. Three of these components exhibited masses in the 23-27 kDa range, whereas the fourth had a mass of about 80 kDa (Table 2). The Mascot hits found at the timeframe where the procoagulant activity was observed suggest that some of these proteins may be SVSPs that are known to exhibit procoagulant ("Thrombin-like enzyme bothrombin"; sequence coverage (SC) of 22%), platelet aggregating ("Platelet-aggregating proteinase PA-BJ"; SC, 49%) or fibrinogenolytic ("Thrombin-like enzyme KN-BJ 2"; SC, 40%) activities. In addition, we detected matches to C-type lectins with known platelet aggregating activities ("Snaclec botrocetin subunit alpha"; SC, 20%) (46), and SVMPs previously described to promote haemorrhage and haemagglutination ("Zinc metalloproteinase-disintegrin-like jararhagin" and "Zinc metalloproteinase/disintegrin"; SC, 46% and 28%, respectively) (40, 46-49).

494 3.3.3 *Calloselasma rhodostoma*

495 In total, four bioactive coagulopathic toxins were detected in the venom of *C. rhodostoma*, one that
496 corresponded to an anticoagulant bioactivity peak, and three to procoagulant peaks (Figure 2C). The
497 anticoagulant correlated to the XIC 1244.1103^{11+} and had a resulting accurate mass of 13665.0848 Da.
498 When comparing this mass with the Mascot search results, this venom toxin was matched to "Inactive basic
499 phospholipase A2 W6D49", a PLA_2 toxin known to cause local oedema but has yet to be described as
500 having anticoagulant activity (50). Similar to those venoms previously described, the XICs could not be
501 correlated to procoagulant bioactivity peaks or Mascot identities. However, the masses of these
502 procoagulant venom toxins were 21-23 kDa and ~28 kDa in size, which suggests that they likely belong to
503 the SVMP or SVSP toxin families. Indeed, the Mascot hits found where procoagulant activity was observed
504 revealed the presence of both these toxin types, along with C-type lectins and an L-amino acid oxidase
505 (Table 2). The SVSP identified ("Thrombin-like enzyme ancrod-2"; SC, 53%) has previously been shown to
506 be fibrinogenolytic (51), while the literature relating to the SVMPs detected ("Snake venom
507 metalloproteinase kistomin" and "Zinc metalloproteinase/disintegrin" SC, 33% and 27%, respectively)
508 suggests they predominately exert anticoagulant activities, including interfering with platelet aggregation
509 and promoting haemorrhage (52, 53). It is therefore possible that these toxins are co-eluting with
510 procoagulant components, although given that many SVMPs are multi-functional proteins that can exert
511 procoagulant bioactivities (54), they may be contributing to the functional effect observed here despite these
512 activities not previously being reported.
513
514 3.3.4 *Daboia russelii*

515 The venom of *D. russelii* exhibited both potent anticoagulant and procoagulant bioactivities (Figure 2D). We
516 identified three XICs that correlated to anticoagulant bioactivity peaks, one of which exhibited a *m/z*-value
517 (1511.6962^{9+}) and could be directly matched to a Mascot identity. This protein had an average mass of
518 13587.2248 Da and corresponded with "Basic phospholipase A2 VRV-PL-VIIIa" (sequence coverage of
519 82%) - a PLA_2 toxin that has been previously described to be anticoagulant (36). Of the remaining
520 anticoagulant XICs, one exhibited a mass of 13649.2513 Da (*m/z*-value 1518.5946^{9+}) and could be
521 correlated to "Basic phospholipase A2 3" (55) exhibiting a mass ~14 Da higher than the PLA2 toxin, and

this slight difference may be caused by a methylation. , whereas the other protein was much smaller in size (*m/z*-value 1116.5835^{1+}; average mass 1115.5759 Da), and remains unidentified. We identified one XIC (*m/z*-value 1086.3866^{21+}) that correlated with a bioactive procoagulant peak, but were also unable to match this via Mascot database searches. The molecular mass of this venom toxin was 22778.9073 Da, which raises the possibly of it being an SVMP or SVSP toxin.

3.3.5 *Echis ocellatus*

We identified three anticoagulant bioactivity peaks in the venom of *Echis ocellatus* that could be linked to XICs (Figure 2E), and two of these were matched to Mascot hits. Both of these XICs (*m/z*-values of 1537.0489^{9+} and 1541.4718^{9+}) resulted in similar average mass values (13815.3523 Da and 13856.1382) and matched the PLA_2 toxins "Phospholipase A2 homolog" and "Acidic phospholipase A2 5". Despite these identifications, and prior reports of PLA_2s generally exerting anticoagulant activities (16), neither of these *E. ocellatus* PLA_2s have previously been described as anticoagulants (33, 56, 57). Despite the venom from these species being potently procoagulant (7, 58), we only identified one XIC that could be correlated to a procoagulant bioactivity peak. This protein had a *m/z*-value of 1445.8645^{35+} and a corresponding mass of 52015.873 Da, but could not be matched to a Mascot hit. Nonetheless, the mass recovered suggests that this could be a SVMP, particularly since this venom is known to be dominated by this toxin class (33), and has previously been demonstrated to contain P-III SVMPs of ~52 kDa in size (13), and potent procoagaulant SVMPs, such as the ~55 kDa prothrombin activator ecarin (59). Supporting this tentative toxin assignment, Mascot hits at the timeframe of the procoagulant activity identified known procoagulant SVMP toxins ("Zinc metalloproteinase-disintegrin-like EoVMP2" and "Zinc metalloproteinase-disintegrin-like EoMP06" SC, 48% and 23% sequence coverage, respectively) (60, 61), along with two, much small molecular weight, C-type lectins ("Snaclec 1" and "Snaclec CTL-Eoc124" SC, 53% and 31%). "Zinc metalloproteinase-disintegrin-like EoVMP2" is a known prothrombin activator and "Zinc metalloproteinase-disintegrin-like EoMP06" is suspected to activate prothrombin based on its sequence similarity with a prothrombin-activating SVMP of *E. pyramidum leakyi* (Ecarin, A55796, 91% similarity) (60, 61). While it is known that some SVMPs form complexes with CTLs, including the *Echis* prothrombin activator carinactivase (62), it is unlikely that these complexes would remain intact after nanofractionation.

3.3.6 *Dispholidus typus*

The venom of *D. typus* yielded three potential coagulopathic venom toxins, two of which were associated with anticoagulant activity, and the third with procoagulanct effects. Two m/z-values (1516.9114^{9+} and 1055.7351^{8+}; masses, 13634.0965 and 8432.8015 Da) were correlated with the anticoagulants. However, these two venom toxins are closely eluting (Figure 2F) and thus it is possible that only one of these components is responsible for the anticoagulant activity. Based on their molecular weight it is tempting to speculate that this activity likely comes from the ~13 kDa compound, particularly since this mass correlates well with a number of anticoagulants detected from the other venoms under study here (e.g. PLA_2 toxins, 13-14 kDa in size). However, given that *D. typus* is the only colubrid venom investigated in this study, and that colubrid PLA_2s are distinct from those of vipers (24), this hypothesis requires testing in future work. Nonetheless, these findings are interesting because there are no prior reports of *D. typus* venom exhibiting anticoagulant activity, likely because this activity is masked by the net procoagulant activity of this venom (7). The procoagulant peak could be correlated to a mass of ~23 kDa (Table 2). This toxin most likely belongs to the SVMPs family, which are the most dominant toxin type in *D. typus* venom (24), and have previously been described to be responsible for the potent procoagulant activity of this species (63).

3.3.7 *Oxyuranus scutellatus*

Oxyuranus scutellatus is the sole representative of the elapid snake family under study here. As venom toxin composition diverted following the split of vipers from all other caenophidian snakes around 50 million years ago (64), we anticipated identifying a number of toxins types not found in viper venoms. The bioactivity chromatogram revealed a large elution region of anticoagulants,with no distinct peaks (Figure 2F). The m/z-values of eight compounds could be correlated to this anticoagulant region. Two of these (788.1641^{9+} and 1091.8042^{6+}; masses, 6993.2858 and 6536.8065 Da) could be matched via Mascot and were identified as Kunitz-type serine protease inhibitors (Kunitz-type serine protease inhibitor taicotoxin and Kunitz-type serine protease inhibitor scutellin-3) both of which are known to exhibit anticoagulant activities and are abundant components in *O. scutellatus* venom (22, 27, 35). The remaining m/z-values had no associated Mascot match. Two of these unidentified components had molecular masses of 5.5-7.1 kDa and thus may also be anticoagulant Kunitz toxins. However, the remaining four anticoagulant XICs corresponded to molecular

578 masses in the range of ~13-14 kDa, and therefore seem likely to be PLA_2s, particularly since the venom of
579 *O. scutellatus* is rich in this toxin class (22). This assertion is also supported by four known PLA_2s being
580 detected in the timeframe of the observed anticoagulant activity, namely: Basic phospholipase A2 taipoxin
581 alpha chain, Neutral phospholipase A2 homolog taipoxin beta chain 1, Phospholipase A2 OS1 and Neutral
582 phospholipase A2 homolog taipoxin beta chain 2. However, none of these PLA_2s have previously been
583 described to be anticoagulant (65, 66). Despite this, and bearing in mind that elapid PLA_2s are distinct from
584 those of vipers (67), a number of elapid PLA_2s have been demonstrated to exert anticoagulant effects (68,
585 69). Nonetheless, improved separation of these venom toxins, followed by isolation and retesting, is required
586 to confirm these tentative identifications. Two m/z-values were correlated to procoagulants with molecular
587 masses of 21-23 kDa, but neither could be matched to Mascot results, and thus remain unidentified from
588 this study.
589

590 **4. Study limitations**

591 Summarising across the species studied here, we found that many of the anticoagulants detected are likely
592 PLA_2 toxins, as indicated by matching masses for some, and the molecular weights determined by MS for
593 others (i.e. ~13-14 kDa). Contrastingly, only a few of the procoagulant activity peaks observed in the plasma
594 coagulation assay could be assigned to detected masses, and none were identified via Mascot database
595 searches. Most probably, these components are of relatively large molecular mass and are poorly ionized,
596 and transferred under the applied ESI and MS conditions (70). Using more dedicated conditions for intact
597 protein analysis would likely overcome this limitation (71, 72). Masses of compounds that could be
598 correlated to procoagulants ranged from 20 to 80 kDa, with the majority between 21 and 28 kDa.
599 Compounds in this mass range most likely are SVMPs and SVSPs, which contain toxins that have previously
600 been described to exhibit procoagulant activities in many haemotoxic snake venoms (11, 18, 73).
601
602 Although venom toxin enzymes are known to be relatively stable under typical RPLC separation conditions
603 (i.e. exposure to organic solvent), on-column denaturation can occur, particularly in the case of later eluting
604 venom toxins. Moreover, in RPLC, proteins typically yield rather broad peaks (in contrast to peptides) and
605 representatives of multiple toxin families might elute within the same retention time frames due to poor
606 resolution. Examples observed from this study include PLA_2s coeluting with C-type lectins, and SVMPs with
607 SVSPs. Thus, for some of the potential coagulopathic toxins observed, the assignments described earlier
608 are necessarily tentative, as assignment to specific proteins is hindered by co-elution.
609
610 The nanoLC-MS analysis of the tryptic digests of bioactive fractions followed by Mascot database searches
611 did, however, provide a large number of hits, indicating that venom toxins are present but were not
612 previously detected as intact proteins directly after separation by MS. More details regarding the Mascot
613 SwissProt database search is found in the SI. This includes Mascot finding toxins in the seven analysed
614 snakes from different species, which is explained by the fact that there are high sequence similarities for
615 many toxins among different snake species. From all the Mascot data obtained two extensive tables were
616 comprised, one generated from the Uniprot database and the other from the species-specific databases
617 (see SI Species specific databases table and SI Uniprot databases table). There was a significant difference

in recovering components above 20 kDa between the LC-MS-bioassay correlation approach and the nanoLC-MS approach. This was most likely caused due to the lack of sensitivity of the LC-MS caused by poor ionization or insufficient amounts of the proteins, as mentioned before. The nanoLC-MS-Mascot approach was far more sensitive due to the much better ionization of peptides compared to intact proteins. Isolation and further elucidation of the toxins correlated to the bioactivity peaks is necessary for the confirmation of their activity. Finally, it is possible that there could be co-eluting bioactive components that were not detected by MS.

It has to be mentioned that for most of the seven snakes profiled many more Mascot identities were found at the timeframes of the pro- and anticoagulant activities but that mostly only the ones for which a high sequence coverage and/or an accurate mass was established, were mentioned in the text. The venom toxin identities reported are in some cases from different species than analyzed, which means that the possible bioactive compound is not an exact match, but has high sequence similarity to a venom toxin from another snake species of which the transcriptomic data was available in the Mascot database. The sequence similarities between species are causing a high number of search hits in Mascot and this is the reason why not all findings are mentioned in the text but presented in the SI Uniprot databases table.

635 **5. Summary of toxin identifications**

636 Despite these limitations, the at-line nanofractionation approach in combination with the plasma coagulation
637 assay proved to be a fast and powerful approach for the identification of a number of venom toxins that
638 affect the coagulation cascade. Fig 4., provides a summary of the toxins that were detected as being
639 procoagulant and anticoagulant from each of the seven snake venoms studied. For the procoagulant
640 activities, SVMPs, SVSPs and C-type lectins were found in five out of the seven species analysed in depth,
641 while LAAOs were found in three of the seven (Fig 4). These identifications form the basis for future
642 confirmatory studies characterizing the procoagulant activities of the toxins identified here, and for defining
643 those venom components that to not perturb coagulation and were detected here as the result of co-elution.
644 For the anticoagulant activities it became evident that PLA_2s play an important role for all species included
645 in this study, as at least one PLA_2 was detected in each of the seven venoms. In six of the seven venoms
646 analysed we also detected C-type lectins in bioactive regions, although only one of these was associated
647 with anticoagulant activity (in *Oxyuranus scutellatus*). This is perhaps surprising given that C-type lectins
648 are predominately associated with anticoagulant activities (17, 74-78), however, these toxins may perhaps
649 work in a synergistic manner with other toxins, or may not have been associated with anticoagulant activity
650 here, due to many eluting in the procoagulant timeframe of the bioassay, resulting in anticoagulant activities
651 being masked by procoagulant toxins. While the reverse may also happen (e.g. weakly procoagulant toxins
652 being masked via co-eluting in the anticoagulant areas), it is worth noting that one of the strengths of our
653 approach is the deconvolution of coagulopathic toxin activities from the complex venom mixture, and
654 specifically the identification of anticoagulant venom activity from these 'net' procoagulant venoms. Prior
655 studies using crude venom have demonstrated that the majority of the venoms tested here are procoagulant
656 and potently clot plasma (7, 29, 31, 32, 54, 79-82). Despite these observations, our nanofractionation
657 approach clearly reveals that many of these venoms also contain anticoagulant bioactives (e.g. 10 of 20
658 initial venoms, Table 1; 7 of 7 venoms analysed in depth; Figures 1 and 2), which are completely masked
659 when using crude venom in such screening assays.
660

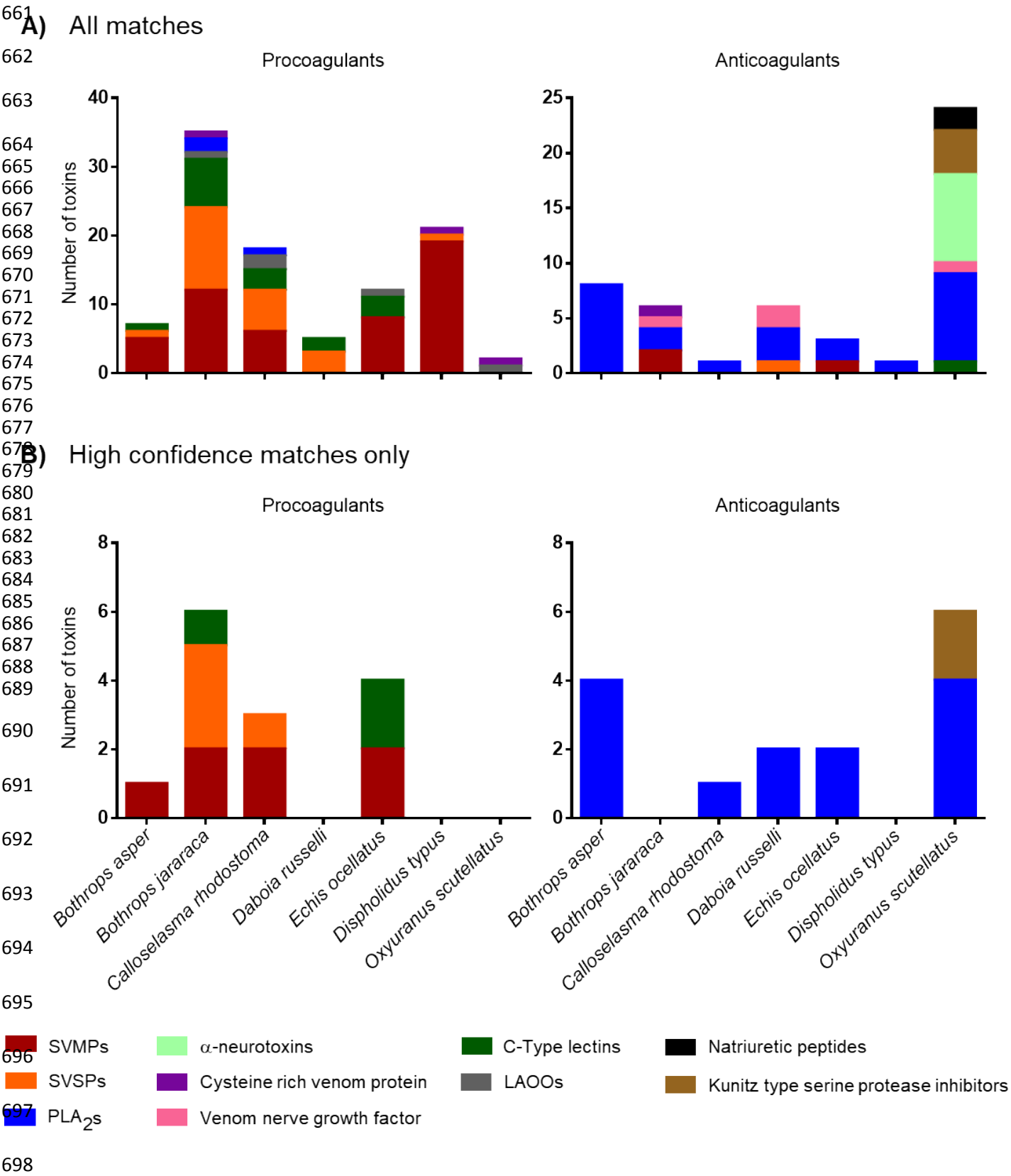

699 **Fig 4. Identification of the various anti- and pro-coagulant toxins associated with the areas in the**
700 **bioactivity profiles where pro- and anti-coagulant activities were observed.** Panel A shows all the
701 toxins found where pro and anticoagulant is observed. This panel is constructed with the SI species specific
702 databases table found in the Supplementary information. Panel B shows toxins that could be matched to
703 observed bioactivity with high confidence due to correlation with MS data or abundance of the toxin and its
704 known activity. This panel is constructed with the data found in Table 2.

705

6. Conclusion

The results of this study describe the validity of using a medium throughput approach for the identification of venom toxins associated with specific pathogenically-relevant bioactivities. In this case, we applied the screening approach to the topic of coagulopathy, as this is well known to be one of the most frequent, serious, pathologies observed following snakebite. The mechanisms of action of coagulopathic snake venom toxins are diverse and can result in both anticoagulant and procoagulant effects. Characterisation of specific target bioactives is challenging though, as venoms are complex mixtures of toxins, therefore methods to deconvolute them are required. The methodology applied here facilitated the rapid identification and fractionation of coagulopathic toxins, which resulted in the identification of anticoagulant venom activities previously being masked by net procoagulant effects of the crude venom, and also detected a number of anticoagulant PLA_2s not previously known to exhibit anticoagulant activities. Success here, alongside the recent development of other small-scale medium-throughput bioassays focused on characterizing other relevant toxin activities (20, 83-86) means that such assays could be used interchangeably for understanding venom function and pathology – ultimately providing a 'bioassay toolkit' for deconvoluting venom mixtures. These approaches will undoubtedly facilitate new research focused on improving snakebite therapy. Current conventional antivenoms are hampered by their low specificity, as they consist of polyclonal antibodies generated via the immunization of animals with snake venom. This process results in only 10-20% of antibodies being specific to venom toxins, with the remainder directed against environmental antigens, and of those specific antibodies only a proportion will actually be specific to the key pathogenic toxins found in any particular venom (87). Thus, much research effort is now focusing upon increasing the specificity of therapies to specific, pathogenically-important, venom toxins, including the novel application of small molecule inhibitors and monoclonal antibodies (88-93). For both these approaches, screening and identification platforms are important for the selection of molecules exhibiting desirable *in vitro* neutralizing profiles from large drug or antibodies libraries. Thus, ultimately, we foresee the application of this methodological platform to greatly enable the future development of new snakebite therapies, by providing a rational screening process that will enable targeted testing of venom toxin neutralization by new inhibitory molecules.

7. Acknowledgements

The authors thank Taline Kazandjian for assistance with statistical analyses, and Paul Rowley for the extraction of snake venoms. This study was supported by: (i) a Sir Henry Dale Fellowship to N.R.C. (200517/Z/16/Z) jointly funded by the Wellcome Trust and Royal Society, and (iii) a UK Medical Research Council funded Research Grant (MR/S00016X/1) to N.R.C. and J.K.

8. References

1. Kasturiratne A, Wickremasinghe AR, de Silva N, Gunawardena NK, Pathmeswaran A, Premaratna R, et al. The global burden of snakebite: a literature analysis and modelling based on regional estimates of envenoming and deaths. PLoS Med. 2008;5(11):e218.
2. Habib AG, Kuznik A, Hamza M, Abdullahi MI, Chedi BA, Chippaux JP, et al. Snakebite is Under Appreciated: Appraisal of Burden from West Africa. PLoS Negl Trop Dis. 2015;9(9):e0004088.
3. Chippaux JP. Snake-bites: appraisal of the global situation. Bull World Health Organ. 1998;76(5):515-24.
4. Gutierrez JM, Calvete JJ, Habib AG, Harrison RA, Williams DJ, Warrell DA. Snakebite envenoming. Nat Rev Dis Primers. 2017;3:17079.
5. Slagboom J, Kool J, Harrison RA, Casewell NR. Haemotoxic snake venoms: their functional activity, impact on snakebite victims and pharmaceutical promise. Br J Haematol. 2017;177(6):947-59.
6. Harrison RA, Oluoch GO, Ainsworth S, Alsolaiss J, Bolton F, Arias AS, et al. Preclinical antivenom-efficacy testing reveals potentially disturbing deficiencies of snakebite treatment capability in East Africa. PLoS Negl Trop Dis. 2017;11(10):e0005969.
7. Ainsworth S, Slagboom J, Alomran N, Pla D, Alhamdi Y, King SI, et al. The paraspecific neutralisation of snake venom induced coagulopathy by antivenoms. Commun Biol. 2018;1:34.
8. de Silva HA, Ryan NM, de Silva HJ. Adverse reactions to snake antivenom, and their prevention and treatment. Br J Clin Pharmacol. 2016;81(3):446-52.
9. Brown NI. Consequences of neglect: analysis of the sub-Saharan African snake antivenom market and the global context. PLoS Negl Trop Dis. 2012;6(6):e1670.
10. Harrison RA, Cook DA, Renjifo C, Casewell NR, Currier RB, Wagstaff SC. Research strategies to improve snakebite treatment: challenges and progress. J Proteomics. 2011;74(9):1768-80.
11. Kini RM, Koh CY. Metalloproteases Affecting Blood Coagulation, Fibrinolysis and Platelet Aggregation from Snake Venoms: Definition and Nomenclature of Interaction Sites. Toxins (Basel). 2016;8(10).
12. Fry BG, Scheib H, van der Weerd L, Young B, McNaughtan J, Ramjan SF, et al. Evolution of an arsenal: structural and functional diversification of the venom system in the advanced snakes (Caenophidia). Mol Cell Proteomics. 2008;7(2):215-46.
13. Casewell NR, Wagstaff SC, Wuster W, Cook DA, Bolton FM, King SI, et al. Medically important differences in snake venom composition are dictated by distinct postgenomic mechanisms. Proc Natl Acad Sci U S A. 2014;111(25):9205-10.
14. Chippaux JP, Williams V, White J. Snake venom variability: methods of study, results and interpretation. Toxicon. 1991;29(11):1279-303.
15. Maduwage K, Isbister GK. Current treatment for venom-induced consumption coagulopathy resulting from snakebite. PLoS Negl Trop Dis. 2014;8(10):e3220.
16. Kini RM, Evans HJ. Structure-function relationships of phospholipases. The anticoagulant region of phospholipases A2. J Biol Chem. 1987;262(30):14402-7.
17. Morita T. Structures and functions of snake venom CLPs (C-type lectin-like proteins) with anticoagulant-, procoagulant-, and platelet-modulating activities. Toxicon. 2005;45(8):1099-114.
18. Kini RM. Serine proteases affecting blood coagulation and fibrinolysis from snake venoms. Pathophysiol Haemo T. 2005;34(4-5):200-4.
19. Still KS, J.;. Multipurpose HTS Coagulation Analysis: Assay Development and Assessment of Coagulopathic Snake Venoms. Toxins (Basel). 2017;9(12).

20. Mladic M, Zietek BM, Iyer JK, Hermarij P, Niessen WM, Somsen GW, et al. At-line nanofractionation with parallel mass spectrometry and bioactivity assessment for the rapid screening of thrombin and factor Xa inhibitors in snake venoms. Toxicon. 2016;110:79-89.
21. Mladic M, de Waal T, Burggraaff L, Slagboom J, Somsen GW, Niessen WMA, et al. Rapid screening and identification of ACE inhibitors in snake venoms using at-line nanofractionation LC-MS. Anal Bioanal Chem. 2017.
22. Herrera M, Fernandez J, Vargas M, Villalta M, Segura A, Leon G, et al. Comparative proteomic analysis of the venom of the taipan snake, Oxyuranus scutellatus, from Papua New Guinea and Australia: role of neurotoxic and procoagulant effects in venom toxicity. J Proteomics. 2012;75(7):2128-40.
23. Thakur R, Chattopadhyay P, Ghosh SS, Mukherjee AK. Elucidation of procoagulant mechanism and pathophysiological significance of a new prothrombin activating metalloprotease purified from Daboia russelii russelii venom. Toxicon. 2015;100:1-12.
24. Pla D, Sanz L, Whiteley G, Wagstaff SC, Harrison RA, Casewell NR, et al. What killed Karl Patterson Schmidt? Combined venom gland transcriptomic, venomic and antivenomic analysis of the South African green tree snake (the boomslang), Dispholidus typus. Biochim Biophys Acta Gen Subj. 2017;1861(4):814-23.
25. Wagstaff SC, Harrison RA. Venom gland EST analysis of the saw-scaled viper, Echis ocellatus, reveals novel alpha9beta1 integrin-binding motifs in venom metalloproteinases and a new group of putative toxins, renin-like aspartic proteases. Gene. 2006;377:21-32.
26. Junqueira-de-Azevedo IL, Bastos CM, Ho PL, Luna MS, Yamanouye N, Casewell NR. Venom-related transcripts from Bothrops jararaca tissues provide novel molecular insights into the production and evolution of snake venom. Mol Biol Evol. 2015;32(3):754-66.
27. St Pierre L, Earl ST, Filippovich I, Sorokina N, Masci PP, De Jersey J, et al. Common evolution of waprin and kunitz-like toxin families in Australian venomous snakes. Cell Mol Life Sci. 2008;65(24):4039-54.
28. Wobbrock J, Findlater L, Gergle D, Higgins J. Proceedings of the ACM Conference on Human Factors in Computing Systems. The Aligned Rank Transform for nonparametric factorial analyses using only ANOVA procedures: ACM Press New York; 2011.
29. Sousa LF, Zdenek CN, Dobson JS, Op den Brouw B, Coimbra F, Gillett A, et al. Coagulotoxicity of Bothrops (Lancehead Pit-Vipers) Venoms from Brazil: Differential Biochemistry and Antivenom Efficacy Resulting from Prey-Driven Venom Variation. Toxins (Basel). 2018;10(10).
30. Debono J, Dobson J, Casewell NR, Romilio A, Li B, Kurniawan N, et al. Coagulating Colubrids: Evolutionary, Pathophysiological and Biodiscovery Implications of Venom Variations between Boomslang (Dispholidus typus) and Twig Snake (Thelotornis mossambicanus). Toxins (Basel). 2017;9(5).
31. Bjarnason JB, Fox JW. Hemorrhagic metalloproteinases from snake venoms. Pharmacol Ther. 1994;62(3):325-72.
32. Takeya H, Nishida S, Miyata T, Kawada S, Saisaka Y, Morita T, et al. Coagulation factor X activating enzyme from Russell's viper venom (RVV-X). A novel metalloproteinase with disintegrin (platelet aggregation inhibitor)-like and C-type lectin-like domains. J Biol Chem. 1992;267(20):14109-17.
33. Wagstaff SC, Sanz L, Juarez P, Harrison RA, Calvete JJ. Combined snake venomics and venom gland transcriptomic analysis of the ocellated carpet viper, Echis ocellatus. J Proteomics. 2009;71(6):609-23.
34. Tang EL, Tan CH, Fung SY, Tan NH. Venomics of Calloselasma rhodostoma, the Malayan pit viper: A complex toxin arsenal unraveled. J Proteomics. 2016;148:44-56.
35. Earl ST, Richards R, Johnson LA, Flight S, Anderson S, Liao A, et al. Identification and characterisation of Kunitz-type plasma kallikrein inhibitors unique to Oxyuranus sp. snake venoms. Biochimie. 2012;94(2):365-73.

832 36. Faure G, Gowda VT, Maroun RC. Characterization of a human coagulation factor Xa-binding site
833 on Viperidae snake venom phospholipases A2 by affinity binding studies and molecular bioinformatics.
834 BMC Struct Biol. 2007;7:82.
835 37. Moura-da-Silva AM, Paine MJ, Diniz MR, Theakston RD, Crampton JM. The molecular cloning of a
836 phospholipase A2 from Bothrops jararacussu snake venom: evolution of venom group II phospholipase
837 A2's may imply gene duplications. J Mol Evol. 1995;41(2):174-9.
838 38. Lizano S, Lambeau G, Lazdunski M. Cloning and cDNA sequence analysis of Lys(49) and Asp(49)
839 basic phospholipase A(2) myotoxin isoforms from Bothrops asper. Int J Biochem Cell Biol.
840 2001;33(2):127-32.
841 39. Watanabe L, Vieira DF, Bortoleto RK, Arni RK. Crystallization of bothrombin, a fibrinogen-
842 converting serine protease isolated from the venom of Bothrops jararaca. Acta Crystallogr D Biol
843 Crystallogr. 2002;58(Pt 6 Pt 2):1036-8.
844 40. Serrano SM, Hagiwara Y, Murayama N, Higuchi S, Mentele R, Sampaio CA, et al. Purification and
845 characterization of a kinin-releasing and fibrinogen-clotting serine proteinase (KN-BJ) from the venom of
846 Bothrops jararaca, and molecular cloning and sequence analysis of its cDNA. Eur J Biochem.
847 1998;251(3):845-53.
848 41. Gutierrez JM, Romero M, Diaz C, Borkow G, Ovadia M. Isolation and characterization of a
849 metalloproteinase with weak hemorrhagic activity from the venom of the snake Bothrops asper
850 (terciopelo). Toxicon. 1995;33(1):19-29.
851 42. Nishida S, Fujimura Y, Miura S, Ozaki Y, Usami Y, Suzuki M, et al. Purification and characterization
852 of bothrombin, a fibrinogen-clotting serine protease from the venom of Bothrops jararaca. Biochemistry.
853 1994;33(7):1843-9.
854 43. Francis B, Gutierrez JM, Lomonte B, Kaiser, II. Myotoxin II from Bothrops asper (Terciopelo)
855 venom is a lysine-49 phospholipase A2. Arch Biochem Biophys. 1991;284(2):352-9.
856 44. Borgheresi RA, Dalle Lucca J, Carmona E, Picarelli ZP. Isolation and identification of angiotensin-
857 like peptides from the plasma of the snake Bothrops jararaca. Comp Biochem Physiol B Biochem Mol
858 Biol. 1996;113(3):467-73.
859 45. Ianzer D, Konno K, Marques-Porto R, Vieira Portaro FC, Stocklin R, Martins de Camargo AC, et al.
860 Identification of five new bradykinin potentiating peptides (BPPs) from Bothrops jararaca crude venom
861 by using electrospray ionization tandem mass spectrometry after a two-step liquid chromatography.
862 Peptides. 2004;25(7):1085-92.
863 46. Fukuda K, Doggett T, Laurenzi IJ, Liddington RC, Diacovo TG. The snake venom protein botrocetin
864 acts as a biological brace to promote dysfunctional platelet aggregation. Nat Struct Mol Biol.
865 2005;12(2):152-9.
866 47. Serrano SM, Mentele R, Sampaio CA, Fink E. Purification, characterization, and amino acid
867 sequence of a serine proteinase, PA-BJ, with platelet-aggregating activity from the venom of Bothrops
868 jararaca. Biochemistry. 1995;34(21):7186-93.
869 48. Fernandez JH, Silva CA, Assakura MT, Camargo AC, Serrano SM. Molecular cloning, functional
870 expression, and molecular modeling of bothrostatin, a new highly active disintegrin from Bothrops
871 jararaca venom. Biochem Biophys Res Commun. 2005;329(2):457-64.
872 49. Escalante T, Nunez J, Moura da Silva AM, Rucavado A, Theakston RD, Gutierrez JM. Pulmonary
873 hemorrhage induced by jararhagin, a metalloproteinase from Bothrops jararaca snake venom. Toxicol
874 Appl Pharmacol. 2003;193(1):17-28.
875 50. Tsai IH, Wang YM, Au LC, Ko TP, Chen YH, Chu YF. Phospholipases A2 from Callosellasma
876 rhodostoma venom gland cloning and sequencing of 10 of the cDNAs, three-dimensional modelling and
877 chemical modification of the major isozyme. Eur J Biochem. 2000;267(22):6684-91.

878 51. Au LC, Lin SB, Chou JS, Teh GW, Chang KJ, Shih CM. Molecular cloning and sequence analysis of
879 the cDNA for ancrod, a thrombin-like enzyme from the venom of Calloselasma rhodostoma. Biochem J.
880 1993;294 (Pt 2):387-90.
881 52. Au LC, Chou JS, Chang KJ, Teh GW, Lin SB. Nucleotide sequence of a full-length cDNA encoding a
882 common precursor of platelet aggregation inhibitor and hemorrhagic protein from Calloselasma
883 rhodostoma venom. Biochim Biophys Acta. 1993;1173(2):243-5.
884 53. Hsu CC, Wu WB, Chang YH, Kuo HL, Huang TF. Antithrombotic effect of a protein-type I class
885 snake venom metalloproteinase, kistomin, is mediated by affecting glycoprotein Ib-von Willebrand factor
886 interaction. Mol Pharmacol. 2007;72(4):984-92.
887 54. Ferraz CR, Arrahman A, Xie C, Casewell NR, Lewis RJ, Kool J, et al. Multifunctional Toxins in Snake
888 Venoms and Therapeutic Implications: From Pain to Hemorrhage and Necrosis. Frontiers in Ecology and
889 Evolution. 2019;7(218).
890 55. Suzuki M, Itoh T, Anuruddhe BM, Bandaranayake IK, Shirani Ranasinghe JG, Athauda SB, et al.
891 Molecular diversity in venom proteins of the Russell's viper (Daboia russellii russellii) and the Indian
892 cobra (Naja naja) in Sri Lanka. Biomed Res. 2010;31(1):71-81.
893 56. Bharati K, Hasson SS, Oliver J, Laing GD, Theakston RD, Harrison RA. Molecular cloning of
894 phospholipases A(2) from venom glands of Echis carpet vipers. Toxicon. 2003;41(8):941-7.
895 57. Conlon JM, Attoub S, Arafat H, Mechkarska M, Casewell NR, Harrison RA, et al. Cytotoxic
896 activities of [Ser(4)(9)]phospholipase A(2) from the venom of the saw-scaled vipers Echis ocellatus, Echis
897 pyramidum leakeyi, Echis carinatus sochureki, and Echis coloratus. Toxicon. 2013;71:96-104.
898 58. Rogalski A, Soerensen C, Op den Brouw B, Lister C, Dashevsky D, Arbuckle K, et al. Differential
899 procoagulant effects of saw-scaled viper (Serpentes: Viperidae: Echis) snake venoms on human plasma
900 and the narrow taxonomic ranges of antivenom efficacies. Toxicol Lett. 2017;280:159-70.
901 59. Kornalik F, Blomback B. Prothrombin activation induced by Ecarin - a prothrombin converting
902 enzyme from Echis carinatus venom. Thromb Res. 1975;6(1):57-63.
903 60. Hasson SS, Theakston RD, Harrison RA. Cloning of a prothrombin activator-like metalloproteinase
904 from the West African saw-scaled viper, Echis ocellatus. Toxicon. 2003;42(6):629-34.
905 61. Howes JM, Kamiguti AS, Theakston RD, Wilkinson MC, Laing GD. Effects of three novel
906 metalloproteinases from the venom of the West African saw-scaled viper, Echis ocellatus on blood
907 coagulation and platelets. Biochim Biophys Acta. 2005;1724(1-2):194-202.
908 62. Yamada D, Sekiya F, Morita T. Isolation and characterization of carinactivase, a novel
909 prothrombin activator in Echis carinatus venom with a unique catalytic mechanism. J Biol Chem.
910 1996;271(9):5200-7.
911 63. Kamiguti AS, Theakston RD, Sherman N, Fox JW. Mass spectrophotometric evidence for P-III/P-IV
912 metalloproteinases in the venom of the Boomslang (Dispholidus typus). Toxicon. 2000;38(11):1613-20.
913 64. Alencar LRV, Quental TB, Grazziotin FG, Alfaro ML, Martins M, Venzon M, et al. Diversification in
914 vipers: Phylogenetic relationships, time of divergence and shifts in speciation rates. Molecular
915 Phylogenetics and Evolution. 2016;105:50-62.
916 65. Cendron L, Micetic I, Polverino de Laureto P, Paoli M. Structural analysis of trimeric
917 phospholipase A2 neurotoxin from the Australian taipan snake venom. FEBS J. 2012;279(17):3121-35.
918 66. Rouault M, Rash LD, Escoubas P, Boilard E, Bollinger J, Lomonte B, et al. Neurotoxicity and other
919 pharmacological activities of the snake venom phospholipase A2 OS2: the N-terminal region is more
920 important than enzymatic activity. Biochemistry. 2006;45(18):5800-16.
921 67. Doley R, Zhou X, Kini RM. Snake venom phospholipase A2 enzymes. Handbook of venoms and
922 toxins of reptiles. 2010;1:173-205.
923 68. Lalloo DG, Trevett AJ, Black J, Mapao J, Saweri A, Naraqi S, et al. Neurotoxicity, anticoagulant
924 activity and evidence of rhabdomyolysis in patients bitten by death adders (Acanthophis sp.) in southern
925 Papua New Guinea. QJM. 1996;89(1):25-35.

926 69. Sharp PJ, Berry SL, Spence I, Howden ME. A basic phospholipase A from the venom of the
927 Australian king brown snake (Pseudechis australis) showing diverse activities against membranes. Comp
928 Biochem Physiol B. 1989;92(3):501-8.
929 70. Rodriguez-Aller M, Gurny R, Veuthey JL, Guillarme D. Coupling ultra high-pressure liquid
930 chromatography with mass spectrometry: constraints and possible applications. J Chromatogr A.
931 2013;1292:2-18.
932 71. Fort KL, van de Waterbeemd M, Boll D, Reinhardt-Szyba M, Belov ME, Sasaki E, et al. Expanding
933 the structural analysis capabilities on an Orbitrap-based mass spectrometer for large macromolecular
934 complexes. Analyst. 2017;143(1):100-5.
935 72. van de Waterbeemd M, Fort KL, Boll D, Reinhardt-Szyba M, Routh A, Makarov A, et al. High-
936 fidelity mass analysis unveils heterogeneity in intact ribosomal particles. Nat Methods. 2017;14(3):283-6.
937 73. Kini RM, Rao VS, Joseph JS. Procoagulant proteins from snake venoms. Haemostasis. 2001;31(3-
938 6):218-24.
939 74. Jebali J, Bazaa A, Sarray S, Benhaj K, Karboul A, El Ayeb M, et al. C-type lectin protein isoforms of
940 Macrovipera lebetina: cDNA cloning and genetic diversity. Toxicon. 2009;53(2):228-37.
941 75. Ogawa T, Chijiwa T, Oda-Ueda N, Ohno M. Molecular diversity and accelerated evolution of C-
942 type lectin-like proteins from snake venom. Toxicon. 2005;45(1):1-14.
943 76. Morita T. C-type lectin-related proteins from snake venoms. Curr Drug Targets Cardiovasc
944 Haematol Disord. 2004;4(4):357-73.
945 77. Guimaraes-Gomes V, Oliveira-Carvalho AL, Junqueira-de-Azevedo IL, DL SD, Pujol-Luz M, Castro
946 HC, et al. Cloning, characterization, and structural analysis of a C-type lectin from Bothrops insularis (BiL)
947 venom. Arch Biochem Biophys. 2004;432(1):1-11.
948 78. Harrison RA, Oliver J, Hasson SS, Bharati K, Theakston RD. Novel sequences encoding venom C-
949 type lectins are conserved in phylogenetically and geographically distinct Echis and Bitis viper species.
950 Gene. 2003;315:95-102.
951 79. Gutierrez JM, Rucavado A, Escalante T, Diaz C. Hemorrhage induced by snake venom
952 metalloproteinases: biochemical and biophysical mechanisms involved in microvessel damage. Toxicon.
953 2005;45(8):997-1011.
954 80. Tans G, Rosing J. Snake venom activators of factor X: an overview. Haemostasis. 2001;31(3-
955 6):225-33.
956 81. Atoda H, Hyuga M, Morita T. The primary structure of coagulation factor IX/factor X-binding
957 protein isolated from the venom of Trimeresurus flavoviridis. Homology with asialoglycoprotein
958 receptors, proteoglycan core protein, tetranectin, and lymphocyte Fc epsilon receptor for
959 immunoglobulin E. J Biol Chem. 1991;266(23):14903-11.
960 82. Teng CM, Hung ML, Huang TF, Ouyang C. Triwaglerin: a potent platelet aggregation inducer
961 purified from Trimeresurus wagleri snake venom. Biochim Biophys Acta. 1989;992(3):258-64.
962 83. Mladic M, Slagboom J, Kool J, Vonk FJ, van Wezel GP, Richardson MK. Detection and
963 identification of antibacterial proteins in snake venoms using at-line nanofractionation coupled to LC-MS.
964 Toxicon. 2018;155:66-74.
965 84. Mladic M, de Waal T, Burggraaff L, Slagboom J, Somsen GW, Niessen WMA, et al. Rapid
966 screening and identification of ACE inhibitors in snake venoms using at-line nanofractionation LC-MS.
967 Anal Bioanal Chem. 2017;409(25):5987-97.
968 85. Zietek BM, Mayar M, Slagboom J, Bruyneel B, Vonk FJ, Somsen GW, et al. Liquid chromatographic
969 nanofractionation with parallel mass spectrometric detection for the screening of plasmin inhibitors and
970 (metallo)proteinases in snake venoms. Anal Bioanal Chem. 2018;410(23):5751-63.
971 86. Slagboom J, Otvos RA, Cardoso FC, Iyer J, Visser JC, van Doodewaerd BR, et al. Neurotoxicity
972 fingerprinting of venoms using on-line microfluidic AChBP profiling. Toxicon. 2018;148:213-22.

87. Casewell NR, Cook DA, Wagstaff SC, Nasidi A, Durfa N, Wuster W, et al. Pre-clinical assays predict pan-African Echis viper efficacy for a species-specific antivenom. PLoS Negl Trop Dis. 2010;4(10):e851.
88. Albulescu L-O, Hale M, Ainsworth S, Alsolaiss J, Crittenden E, Calvete JJ, et al. Preclinical validation of a repurposed metal chelator as a community-based therapeutic for hemotoxic snakebite. bioRxiv. 2019:717280.
89. Bryan-Quiros W, Fernandez J, Gutierrez JM, Lewin MR, Lomonte B. Neutralizing properties of LY315920 toward snake venom group I and II myotoxic phospholipases A2. Toxicon. 2019;157:1-7.
90. Lewin M, Samuel S, Merkel J, Bickler P. Varespladib (LY315920) Appears to Be a Potent, Broad-Spectrum, Inhibitor of Snake Venom Phospholipase A2 and a Possible Pre-Referral Treatment for Envenomation. Toxins (Basel). 2016;8(9).
91. Knudsen C, Laustsen AH. Recent Advances in Next Generation Snakebite Antivenoms. Trop Med Infect Dis. 2018;3(2).
92. Laustsen AH, Karatt-Vellatt A, Masters EW, Arias AS, Pus U, Knudsen C, et al. Publisher Correction: In vivo neutralization of dendrotoxin-mediated neurotoxicity of black mamba venom by oligoclonal human IgG antibodies. Nat Commun. 2018;9(1):4957.
93. Lee CH, Lee YC, Lee YL, Leu SJ, Lin LT, Chen CC, et al. Single Chain Antibody Fragment against Venom from the Snake Daboia russelii formosensis. Toxins (Basel). 2017;9(11).

9. Supporting Information Legends

SI. SI Fig 1. Correlation of mass spectrometry data with assay data using argatroban, SI Fig 2. Initial screening results of all 20 species included in the study, SI Fig 3. Toxin IDs from the specific and non-specific databases from nanofractionated toxins present in wells and subjected to proteomics.

SI_Species specific databases table. All Mascot hits found with the species specific databases in the area where pro- and anticoagulant activity was observed. Table includes information on masses, retention times, well numbers of the nanofractionated toxins, sequence coverage, protein score, toxin class and coagulation activity.

SI_Uniprot database table. All Mascot hits found with the Uniprot database in the area where pro- and anticoagulant activity was observed. Table includes information on masses, retention times, well numbers of the nanofractionated toxins, sequence coverage, protein score, toxin class and coagulation activity.

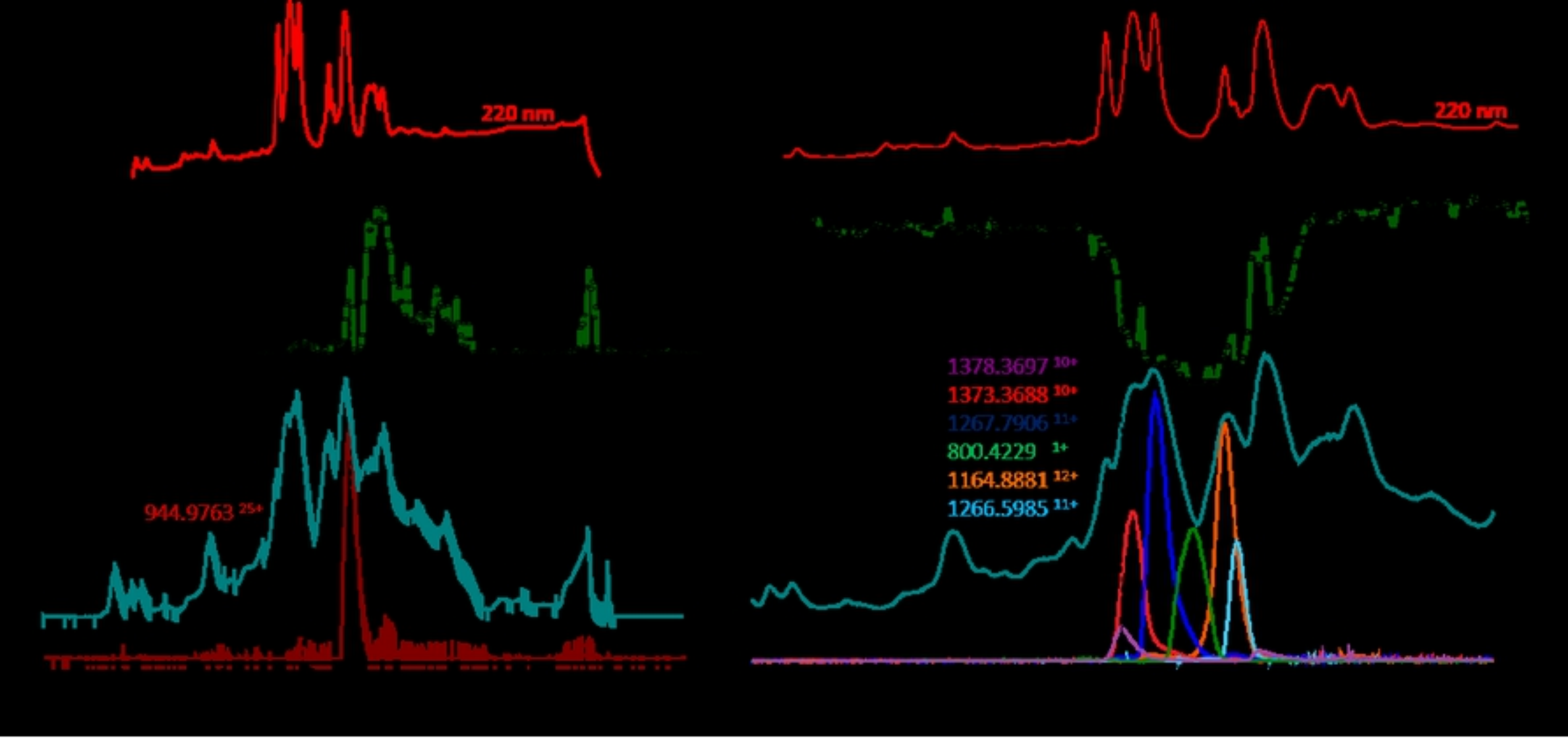
220 nm
220 nm
944.9763 25+
1378.3697 10+
1373.3688 10+
1267.7906 11+
800.4229 1+
1164.8881 12+
1266.5985 11+

Figure

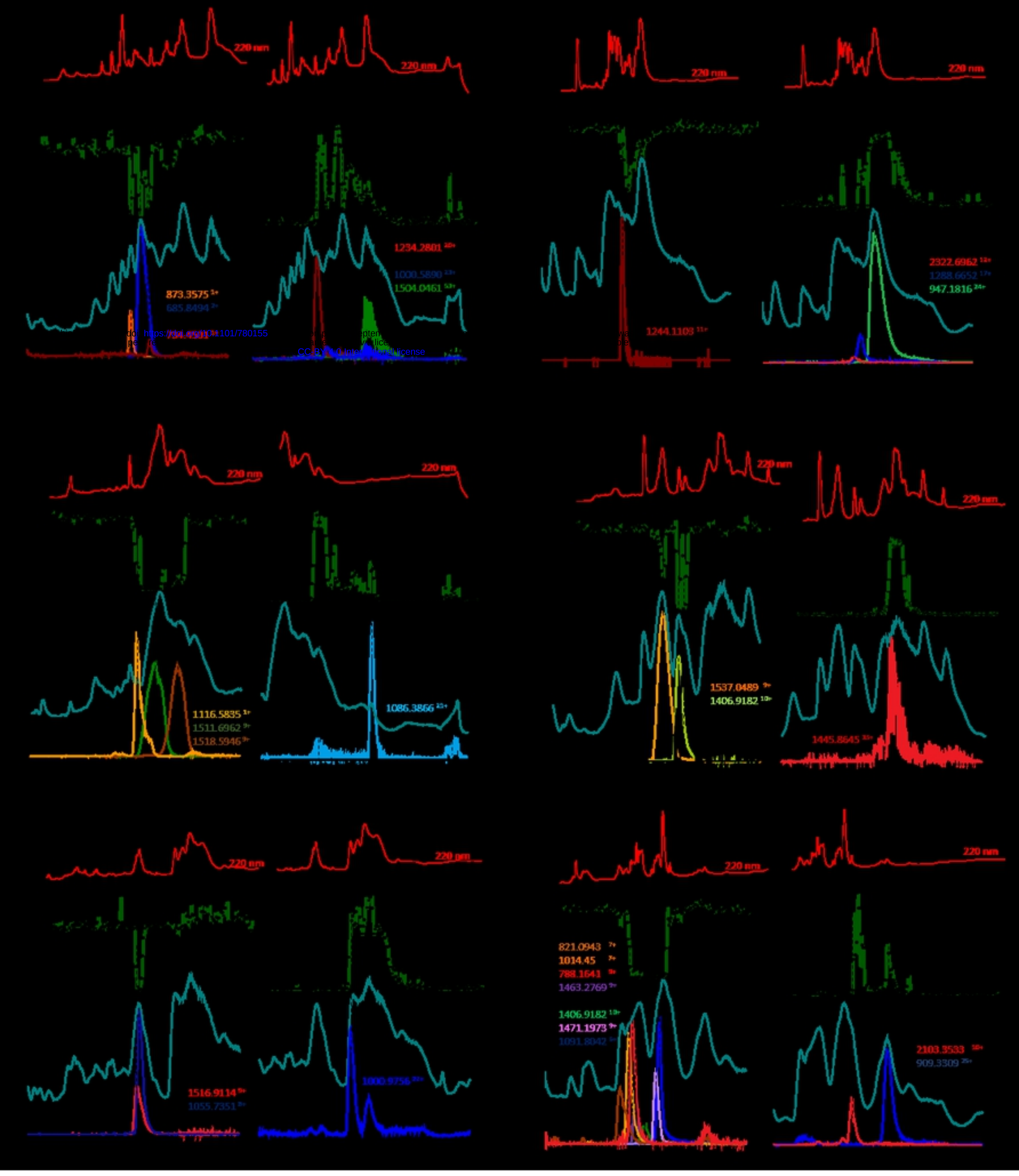

Figure

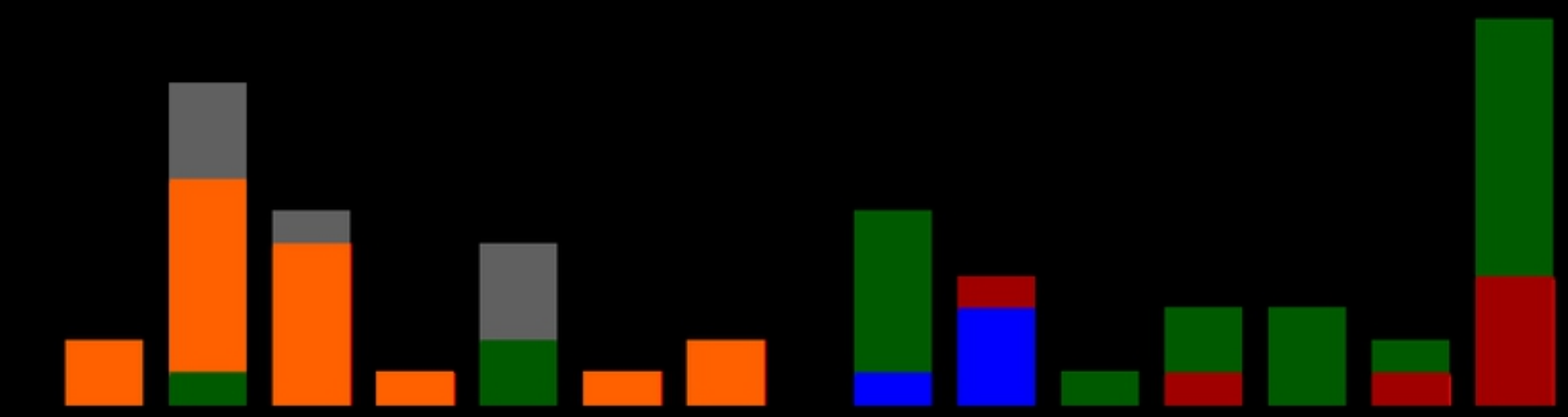

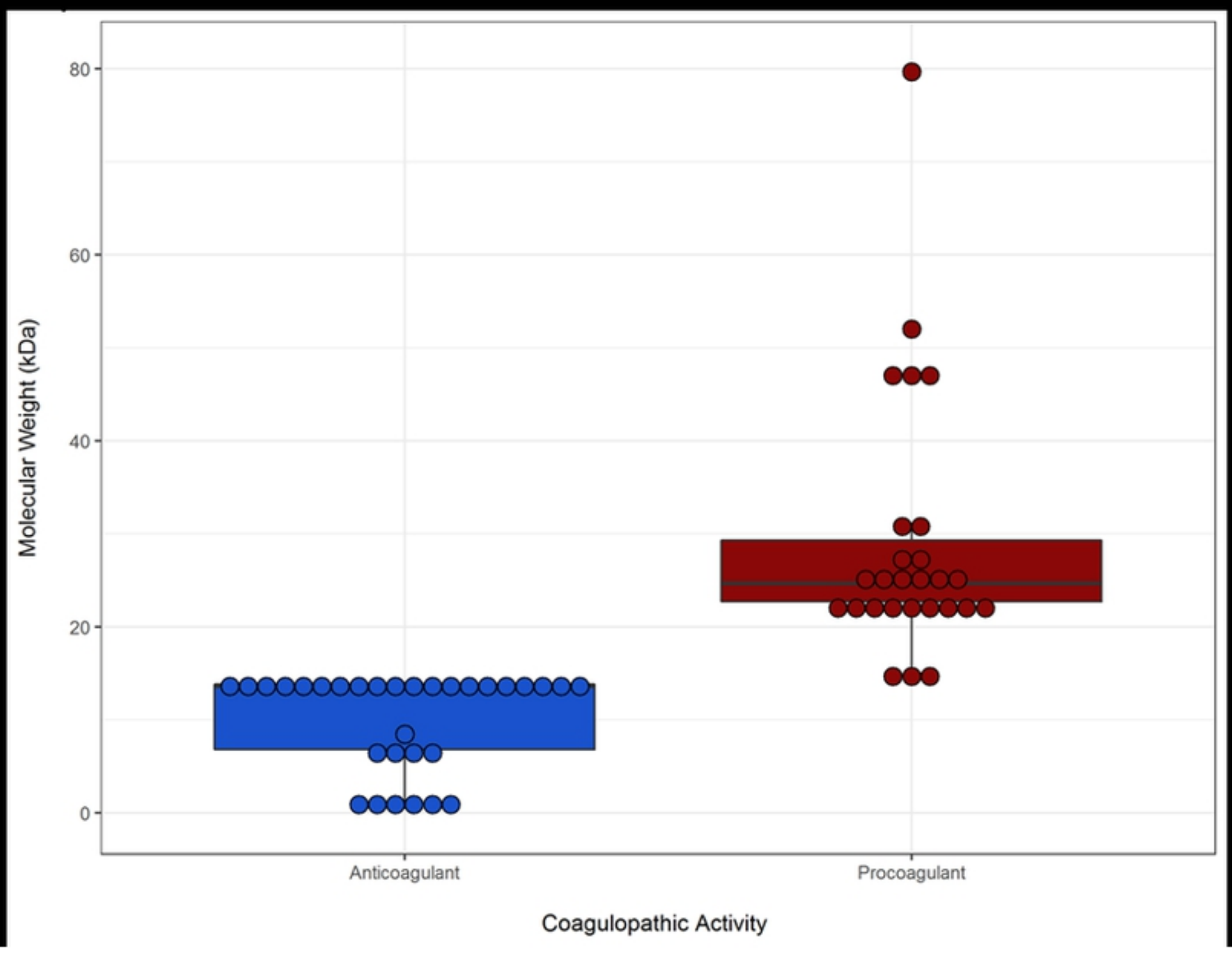

Figure

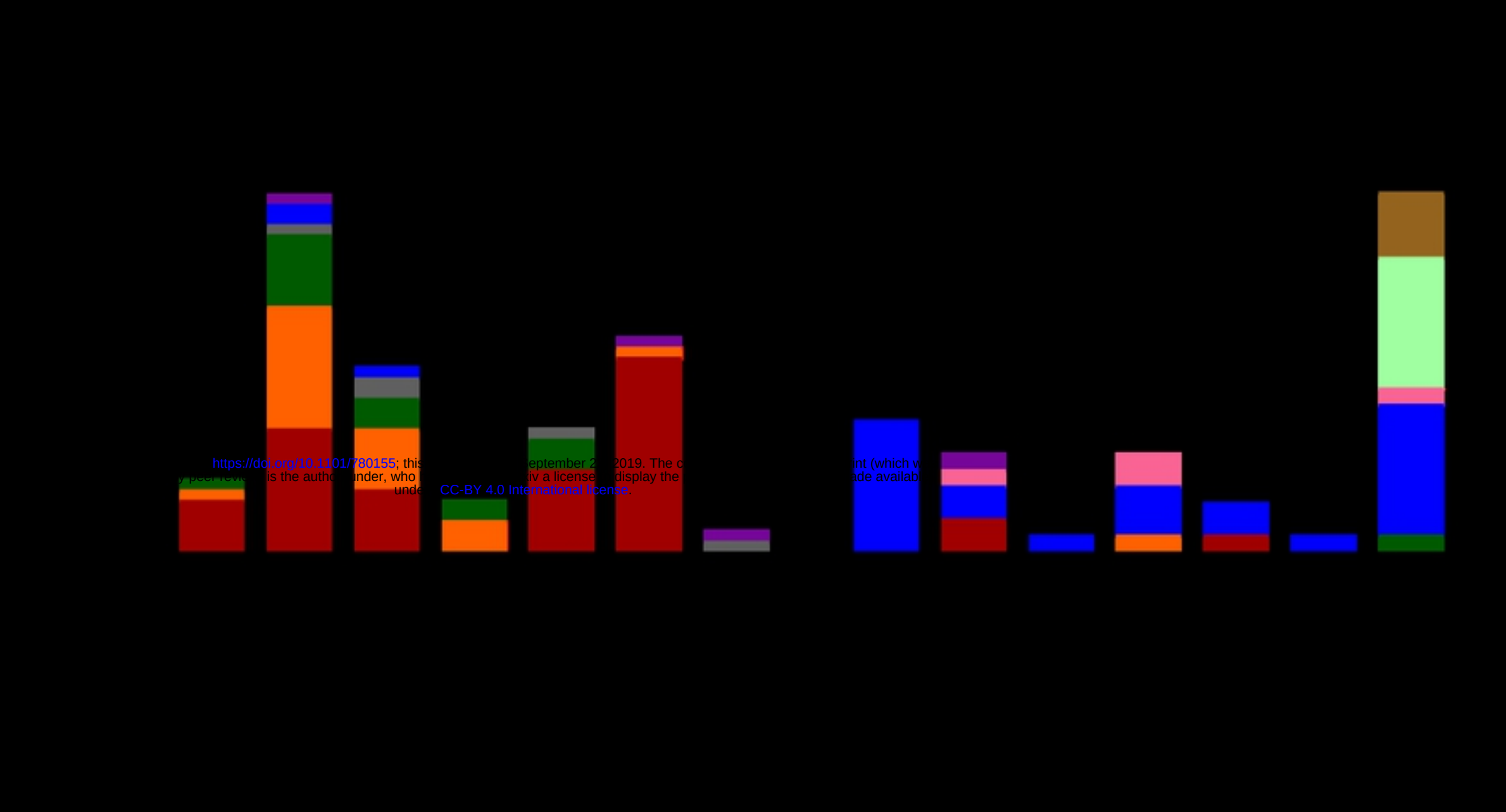

Figure